

# Temperature, carbon dioxide and methane

Clive Hambler (✉ [clive.hamblers@zoo.ox.ac.uk](mailto:clive.hamblers@zoo.ox.ac.uk))

University of Oxford

Peter A. Henderson

University of Oxford

---

## Research Article

**Keywords:** Climate change, Degassing, Outgassing, Productivity, Proxy

**Posted Date:** May 28th, 2021

**DOI:** <https://doi.org/10.21203/rs.3.rs-558940/v1>

**License:**  This work is licensed under a Creative Commons Attribution 4.0 International License.

[Read Full License](#)

---

# 1 **Temperature, carbon dioxide and methane**

2 **Clive Hambler (1)\*, Peter A. Henderson (1,2)**

3

4 (1) Department of Zoology, University of Oxford, UK, ORCID 0000-0002-2361-828X (2) PISCES Conservation  
5 Ltd, UK, ORCID 0000-0002-7461-1758 \* corresponding author clive.hambler@zoo.ox.ac.uk

6

## 7 **Abstract**

8 1) Globally-representative monthly rates of change of atmospheric carbon dioxide and methane are compared with  
9 global rates of change of sea ice and with Arctic and Antarctic air temperatures. 2) Carbon dioxide is very strongly  
10 correlated with sea ice dynamics, with the carbon dioxide rate at Mauna Loa lagging sea ice extent rate by 7 months.  
11 3) Methane is very strongly correlated with sea ice dynamics, with the global (and Mauna Loa) methane rate lagging  
12 sea ice extent rate by 5 months. 4) Sea ice melt rate peaks in very tight synchrony with temperature in each  
13 Hemisphere. 5) The very high synchrony of the two gases is most parsimoniously explained by a common causality  
14 acting in both Hemispheres. 6) Time lags between variables indicate primary drivers of the gas dynamics are due to  
15 solar action on the polar regions, not mid-latitudes as is conventionally believed. 7) Results are consistent with a  
16 proposed role of a high-latitude temperature-dependent abiotic variable such as sea ice in the annual cycles of carbon  
17 dioxide and methane. 8) If sea ice does not drive the net flux of these gases, it is a highly precise proxy for whatever  
18 does. 9) Potential mechanisms should be investigated urgently.

19

20 **Keywords** Climate change • Degassing • Outgassing • Productivity • Proxy

21

22

## 23 **Introduction**

24 The atmospheric levels of carbon dioxide have risen during the instrumental record (IPCC 2013). Superimposed on  
25 the trend are seasonal cycles. At Mauna Loa, Hawaii, carbon dioxide cycles are very regular and levels typically  
26 peak in May of each year, whilst methane, which is less regular, peaks around November. The amplitude of these  
27 cycles is generally highest in northern high latitudes, with some recording sites being exceptions and methane  
28 variation being more complex in the Northern Hemisphere (Fung et al 1991; Dlugokencky et al 1994; He et al 2017,  
29 Dlugokencky et al 2020; Saunio et al 2020; Hambler & Henderson 2020a, b).

30

31 The seasonal cycle of carbon dioxide is typically ascribed to the cycles of terrestrial productivity on the large land  
32 masses of the Northern Hemisphere, generating high seasonal amplitude at Arctic sites such as Barrow and Alert and  
33 with low amplitude at the South Pole and other Antarctic sites (Keeling et al 1989; Keeling et al 2001, 2005;  
34 Buermann et al 2007; Keeling 2008; IPCC 2013; He et al 2017; Jiang & Yung 2019). Similarly, the seasonal  
35 cycle of methane is typically ascribed to the cycle of wetland and agricultural and livestock production (with large  
36 sources on the land masses of the Northern Hemisphere) and to destruction by the OH radical in summer months in  
37 each Hemisphere (Fung et al 1991; Dlugokencky et al 1994).

38

39 However, the seasonal cycles of carbon dioxide and methane are both very strongly correlated with the seasonal  
40 cycle of sea ice, suggesting sea ice could have a dominant causal role in the cycle or is extremely strongly correlated  
41 with whatever does (Hambler & Henderson 2020a, b). This unexpected observation requires explanation and invites  
42 the hypothesis that high-latitude temperature drives the dynamics of these gases. Temperature drives ice melt and  
43 should thus be very highly correlated with the monthly rate of change of these greenhouse gasses - whether or not sea  
44 ice is involved in the cycles. We test this prediction here.

45

46 Temperature is conventionally believed to drive the annual cycles of methane and carbon dioxide through changes in  
47 vegetation and microbial productivity, including agriculture (IPCC 2013). Yet despite great efforts, there is  
48 substantial uncertainty in the locations and magnitudes of sources and sinks for these gases (Kort et al 2012; Zhao et  
49 al 2016; Resplandy et al 2018; Weber et al 2019; Winkler et al 2019; Saunio et al 2020) with polar regions and

50 areas of melting sea ice being amongst the most poorly known due to challenging logistics (Vancoppenolle &  
51 Tedesco 2017; Geilfus et al 2018; Bushinsky et al 2019; MOSAiC 2019).

52

53 The locations of sources and sinks of carbon dioxide have traditionally been estimated using 'inversions' and  
54 'atmospheric transport' models which rely on climate models to reverse-engineer from observed gas levels where  
55 major fluxes occur (*e.g.* Keeling et al 1989; Hein et al 1997; Sitch et al 2015; Zhao et al 2016; Saunois et al 2020).  
56 Similarly, for methane, inversions and machine learning models have predicted where and when major ocean-  
57 atmosphere fluxes occur (such as shallow and Arctic and biologically productive waters) using sparse samples  
58 (Dlugokencky et al 1994; Weber et al 2019; Saunois et al 2020). We suggest an improvement on this method is to  
59 look at the similarity and synchrony of observed monthly rates of change of the gases with observations of potential  
60 causal variables, locally and globally. A dominant causal variable should be most strongly correlated with the global  
61 rate - with least temporal lag between timeseries of the gas rate and its local driver and with co-varying annual  
62 amplitudes. Of course, any seasonal variables such as livestock activity or wetland productivity or sea ice extent will  
63 have correlations with methane and carbon dioxide seasonality, but the spatial pattern of lags between timeseries can  
64 help identify the more likely causes and locations. For example, a polar causal variable should have a relatively high  
65 correlation and low lag with a positive gas flux near the pole.

66

67 Terrestrial productivity in the Northern Hemisphere is typically measured by NDVI (Keeling et al 1989; Keeling et  
68 al 2001; Buermann et al 2007) which is less strongly correlated with carbon dioxide rates than are sea ice rates  
69 (Hambler & Henderson 2020a); to our knowledge no region has been shown to have extremely high temporal  
70 synchrony and hence statistical correlation with the global carbon dioxide rate. Buermann et al (2007) do not present  
71 correlations of  $r > 0.7$ , and include significance values of  $p < 0.1$ . A "strong" correlation coefficient of 0.74 between  
72 the seasonal cycle amplitude of carbon dioxide and Northern Hemisphere land NDVI was detected by He et al  
73 (2017), with the highest local correlations between carbon dioxide levels and NDVI discovered being  $r > 0.9$ .  
74 Oceanic fluxes have been deduced using a grid showing cohesion between temperature anomaly and carbon dioxide  
75 levels at Mauna Loa (Park 2009).

76

77 Given the relatively strong correlations we have found with sea ice (Hambler & Henderson 2020a, b), we predict  
78 very strong synchrony between polar air temperatures and the high latitude fluxes of methane and carbon dioxide

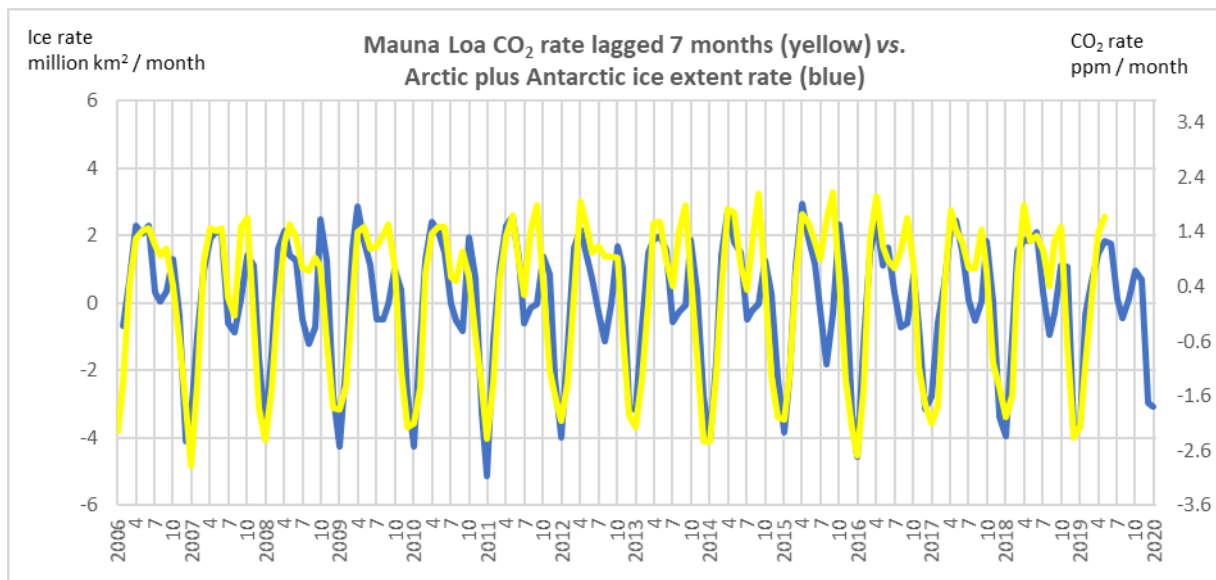
79 (driven mainly by the annual cycle of solar elevation). We hypothesize high-latitude air temperatures drive sea ice  
 80 dynamics and snow dynamics and thence might influence greenhouse gas dynamics. Such strong relationships are  
 81 not presented in the review of the carbon cycle that informs international climate policy (IPCC 2013) and could focus  
 82 greater attention on high latitude sites and fluxes.

83

84 **Results**

85 **a) Globally representative atmospheric gas measurements**

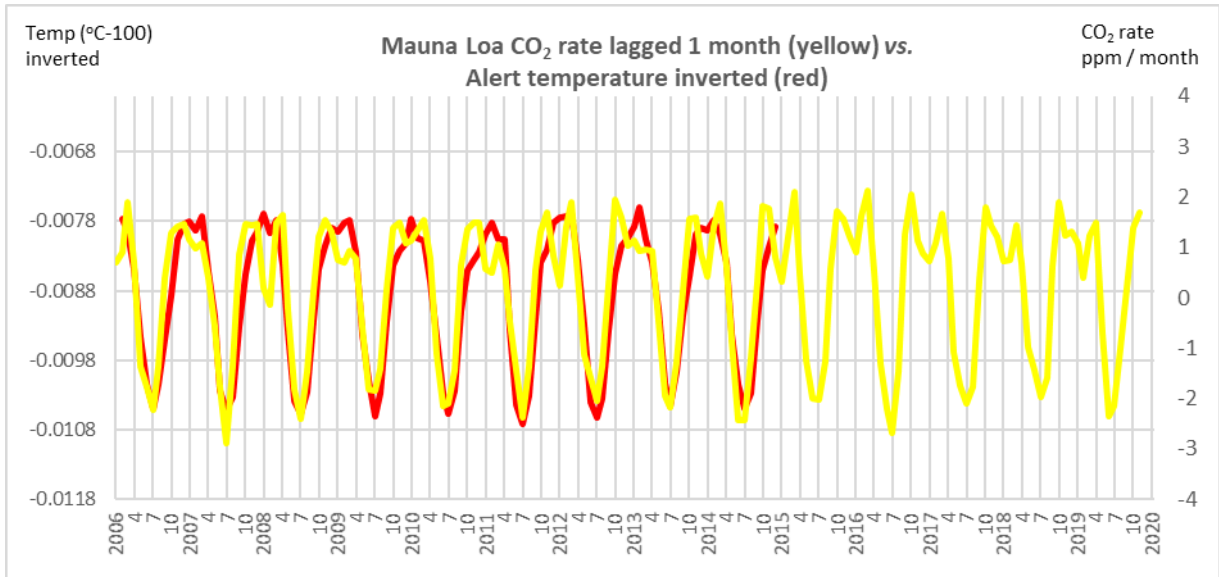
86 The monthly time series for carbon dioxide rate from Mauna Loa, global sea ice extent rate and an Arctic  
 87 temperature (Alert, Canada) are given in Fig. 1 and Fig. 2.



88 **Fig. 1** Global monthly carbon dioxide rate (measured at Mauna Loa, lagged 7 months) vs. global sea ice extent rate.  
 89

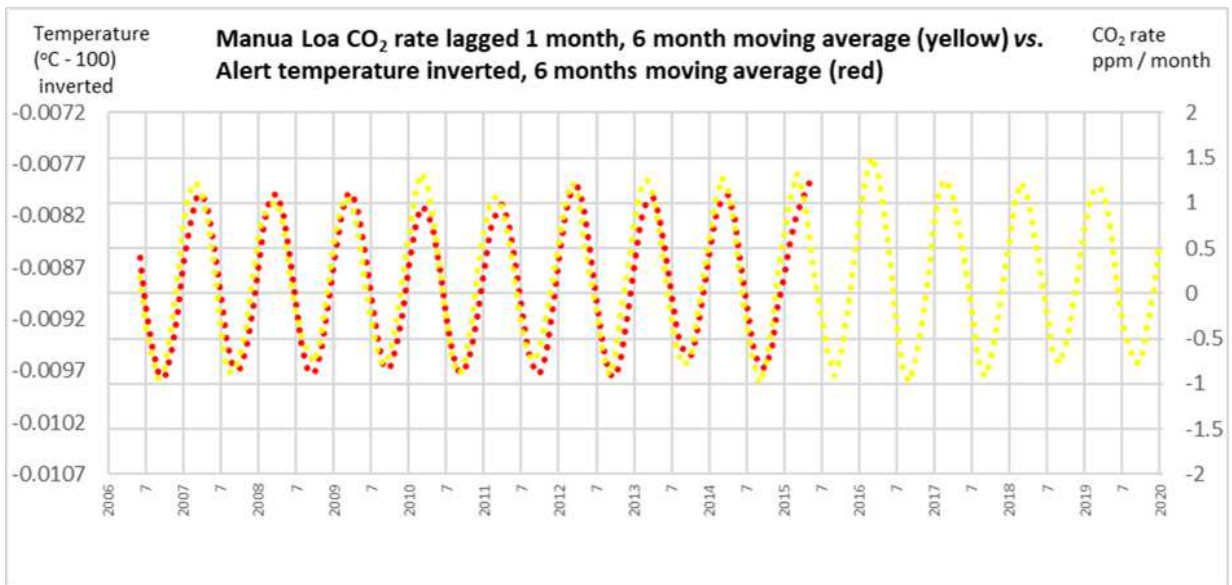
90  $r = 0.79$  at lag = 7 months;  $p < 0.001$

91



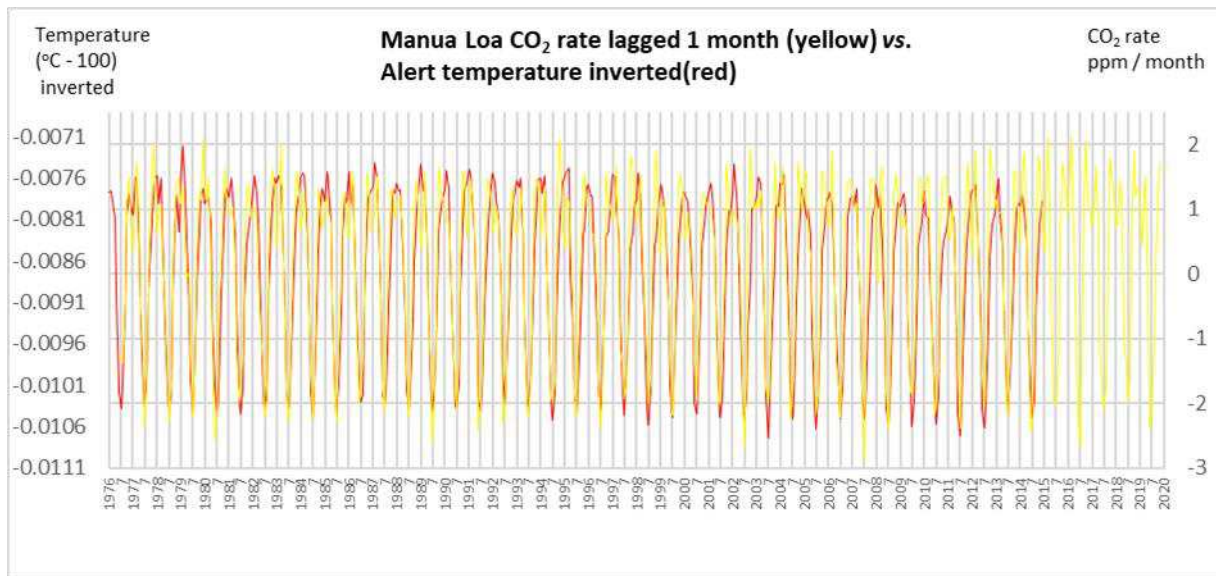
92  
93 **Fig. 2a** Monthly carbon dioxide rate Mauna Loa (lagged 1 month) vs. temperature at Alert (inverted)

94



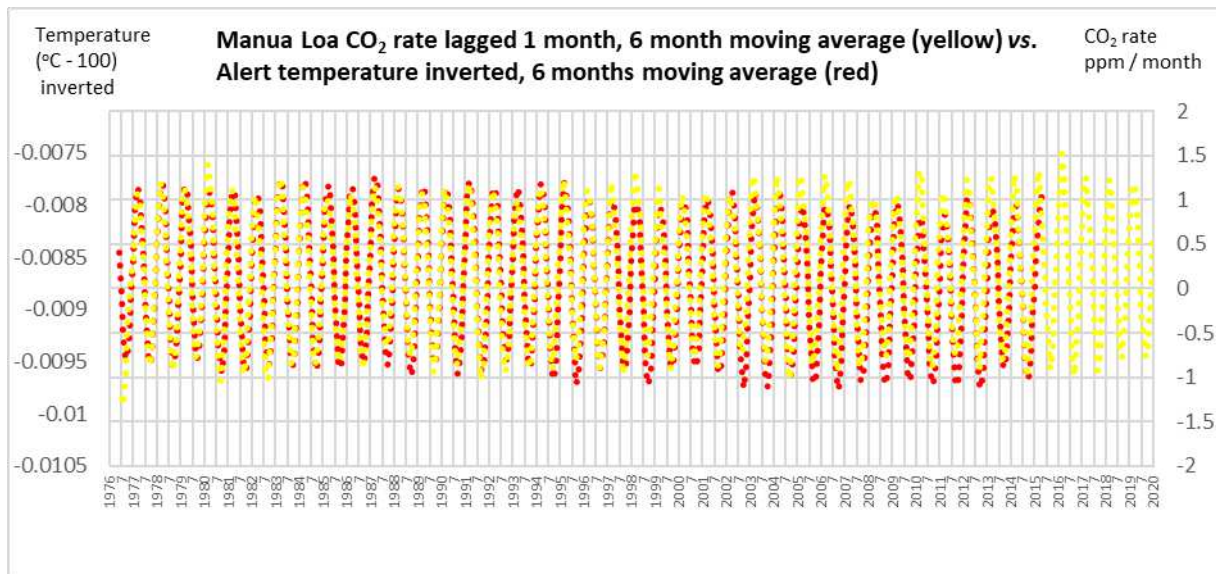
95  
96 **Fig. 2b** Monthly carbon dioxide rate Mauna Loa (lagged 1 months) vs. temperature at Alert, Canada (inverted), 6  
97 month moving average for both variables

98



99  
100 **Fig. 2c** Monthly carbon dioxide rate Mauna Loa (lagged 1 month) vs. temperature at Alert, Canada (inverted), using  
101 full continuous monthly Mauna Loa CO<sub>2</sub> record from July 1976

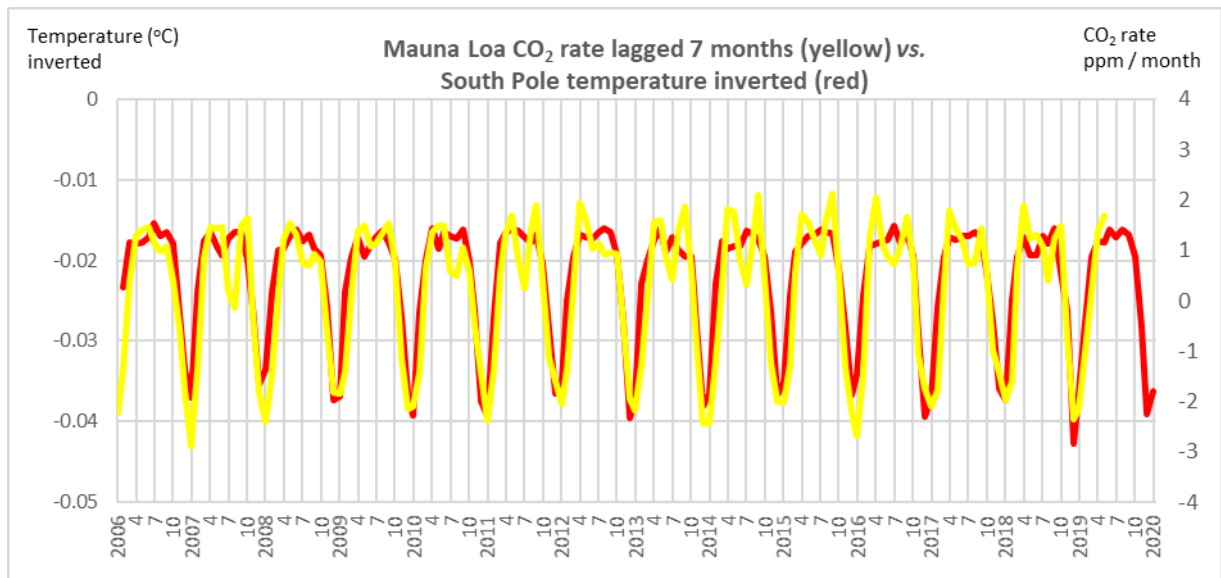
102



103  
104 **Fig. 2d** Monthly carbon dioxide rate Mauna Loa (lagged 1 month) vs. temperature at Alert, Canada (inverted), 6  
105 month moving average for both variables, using full continuous monthly Mauna Loa CO<sub>2</sub> record from July 1976

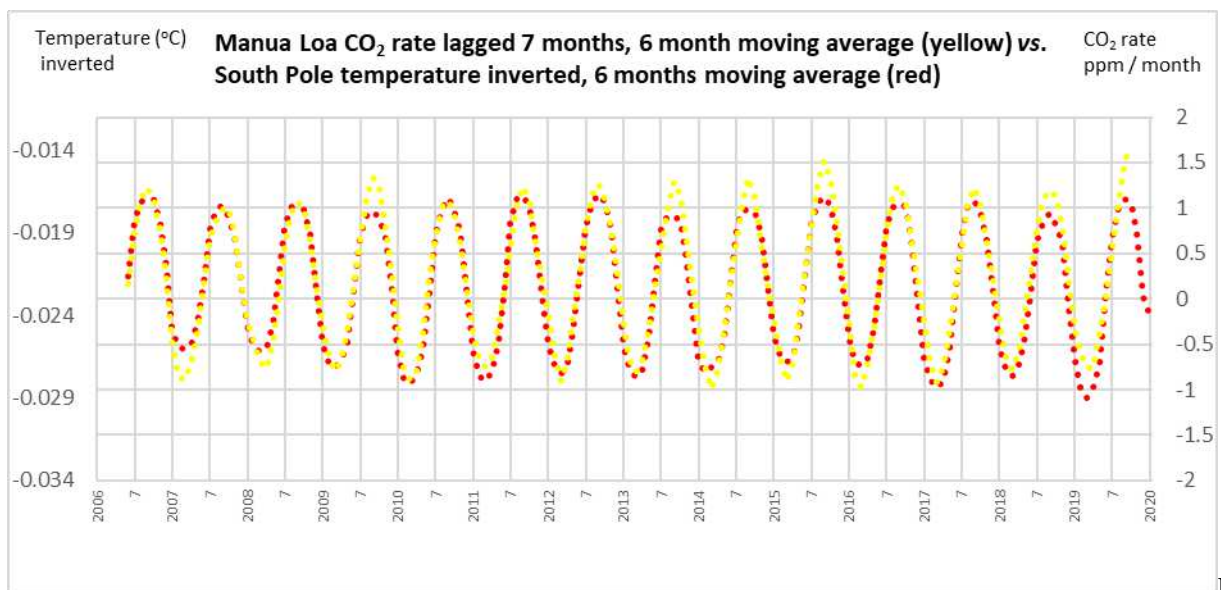
106

107 The monthly time series for carbon dioxide rate from Mauna Loa and an Antarctic temperature (South Pole) are  
108 given in Fig. 3.



109  
110 **Fig. 3a** Monthly carbon dioxide rate Mauna Loa (lagged 7 months) vs. temperature at South Pole (inverted)

111



112 **Fig. 3b** Monthly carbon dioxide rate Mauna Loa (lagged 7 months) vs. temperature at South Pole (inverted), 6 month  
113 moving average for both variables  
114

115

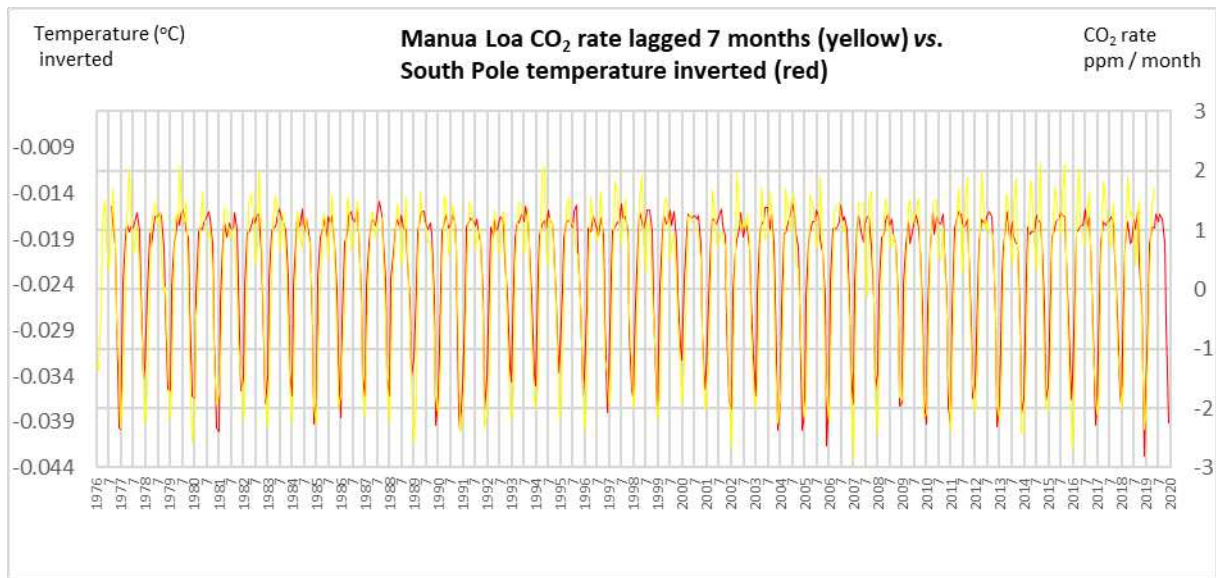
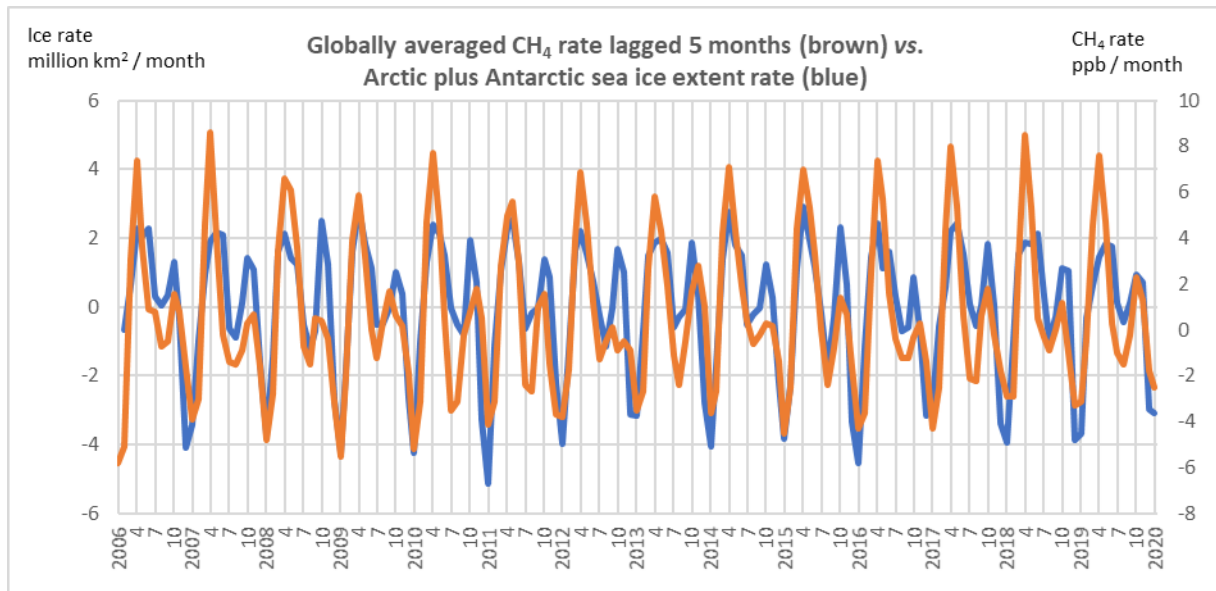


**Fig.**

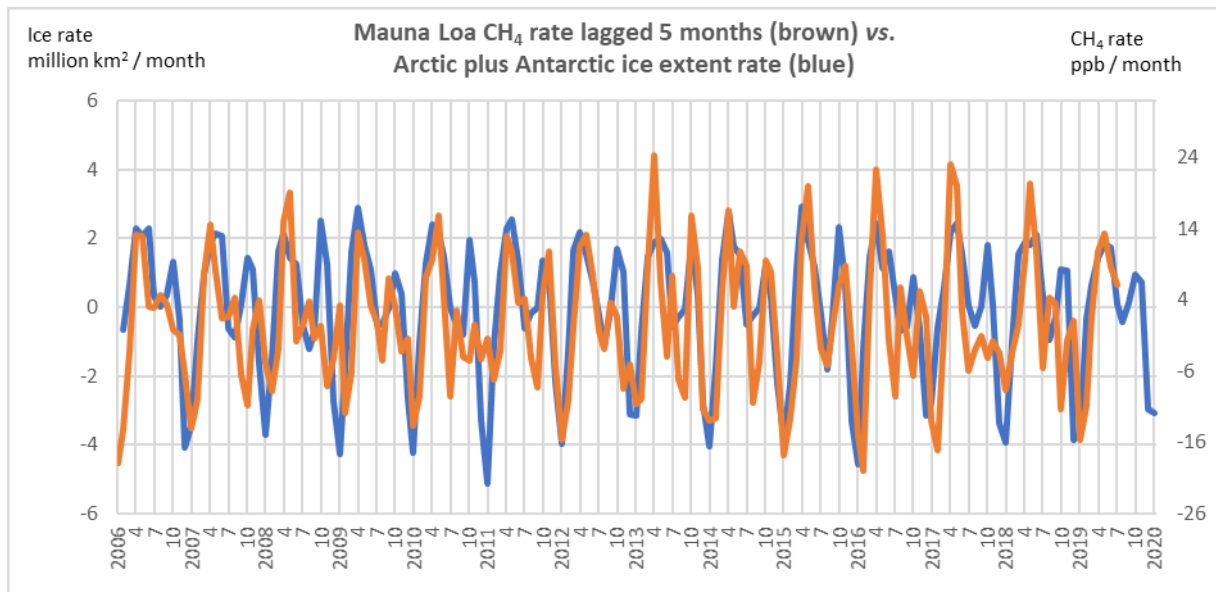
116  
 117 **3c** Monthly carbon dioxide rate Mauna Loa (lagged 7 months) vs. temperature at South Pole (inverted), using full  
 118 continuous monthly Mauna Loa CO<sub>2</sub> record from July 1976

119  
 120 The monthly time series for methane rates averaged from a global network of sites, and from Mauna Loa, are plotted  
 121 against global sea ice extent rate in Fig. 4 and Fig. 5.



122 **Fig. 4** Monthly global average methane rate (lagged 5 months) vs. global sea ice extent rate.  $r = 0.78$  at lag = 5  
 123 months;  $p < 0.001$   
 124

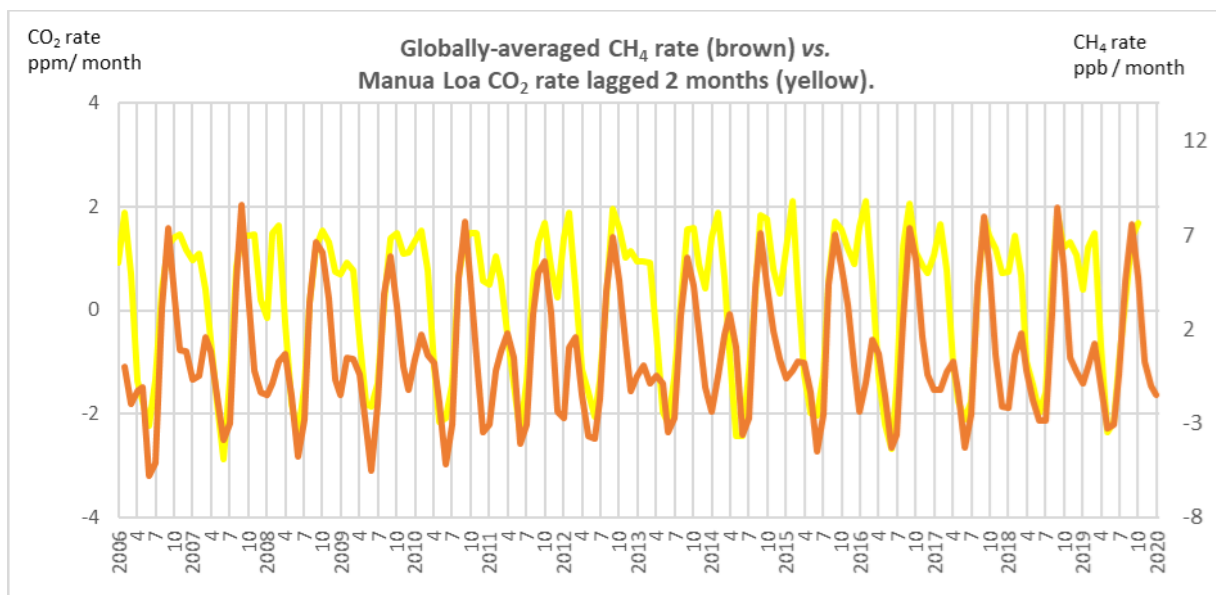
125



126  
127 **Fig. 5** Monthly methane rate Mauna Loa (lagged 5 months) vs. global sea ice extent rate

128

129 Globally representative carbon dioxide and methane rates are compared in Fig. 6.

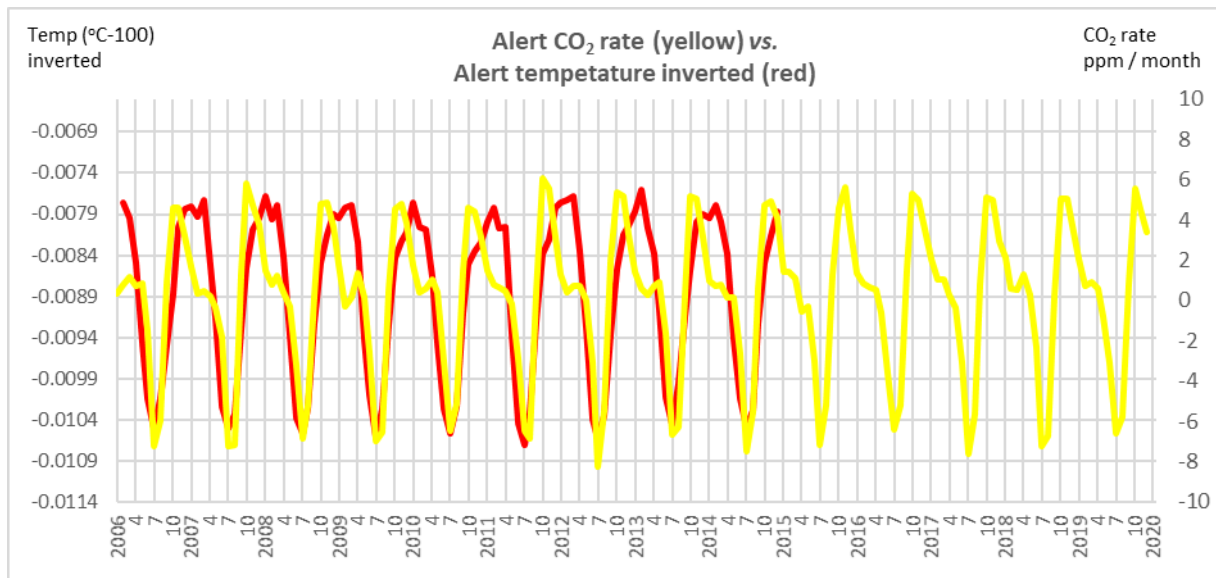


130  
131 **Fig. 6** Global carbon dioxide rate (Mauna Loa, lagged 2 months) vs. global methane rate

132

133 **b) Arctic.** Monthly time series for carbon dioxide and methane rates at Alert (Canada) plotted against Alert

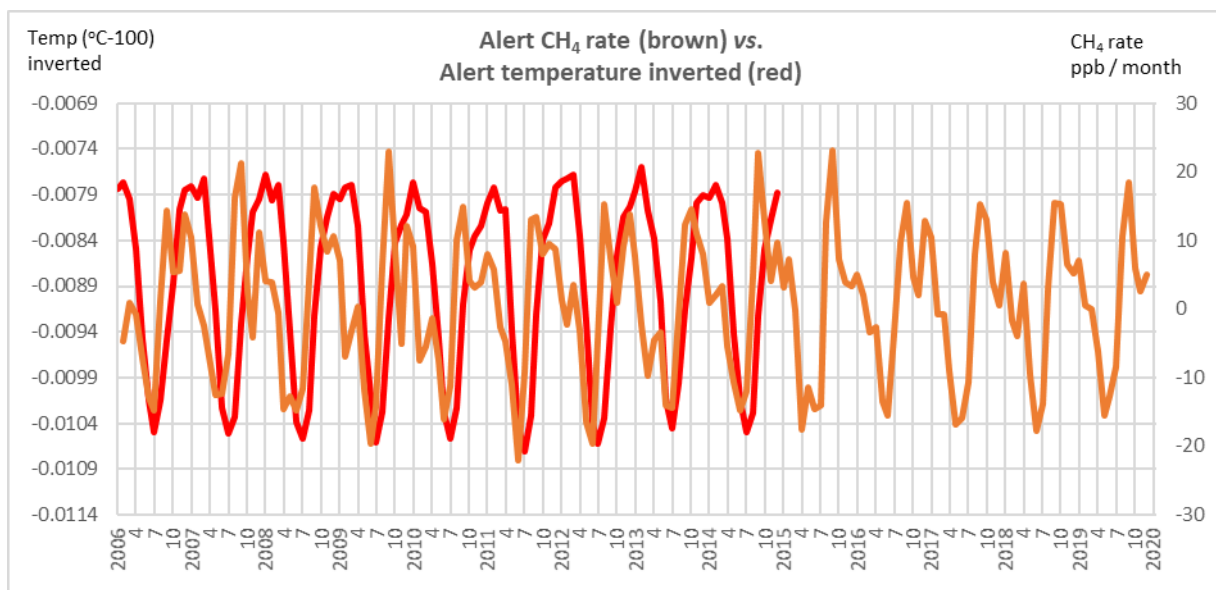
134 temperature and Northern Hemisphere snow extent rate, are given in Figs. 7 - 9.



135  
136

**Fig. 7** Monthly carbon dioxide rate Alert vs. temperature at Alert (inverted)

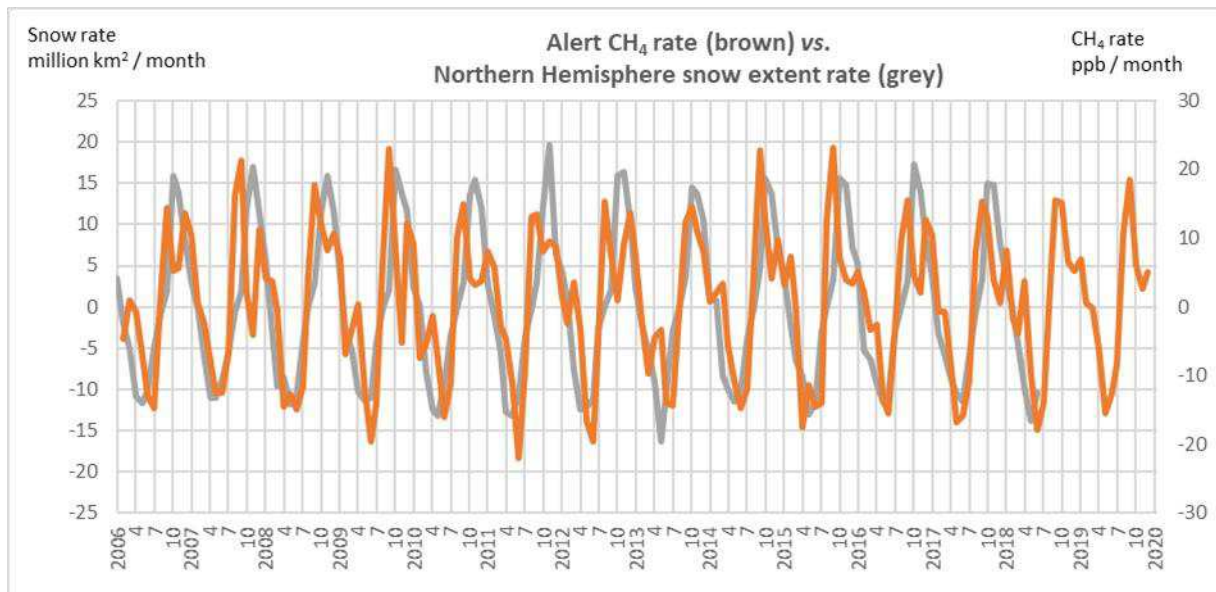
137



138  
139

**Fig. 8** Monthly methane rate Alert vs. temperature at Alert (inverted)

140

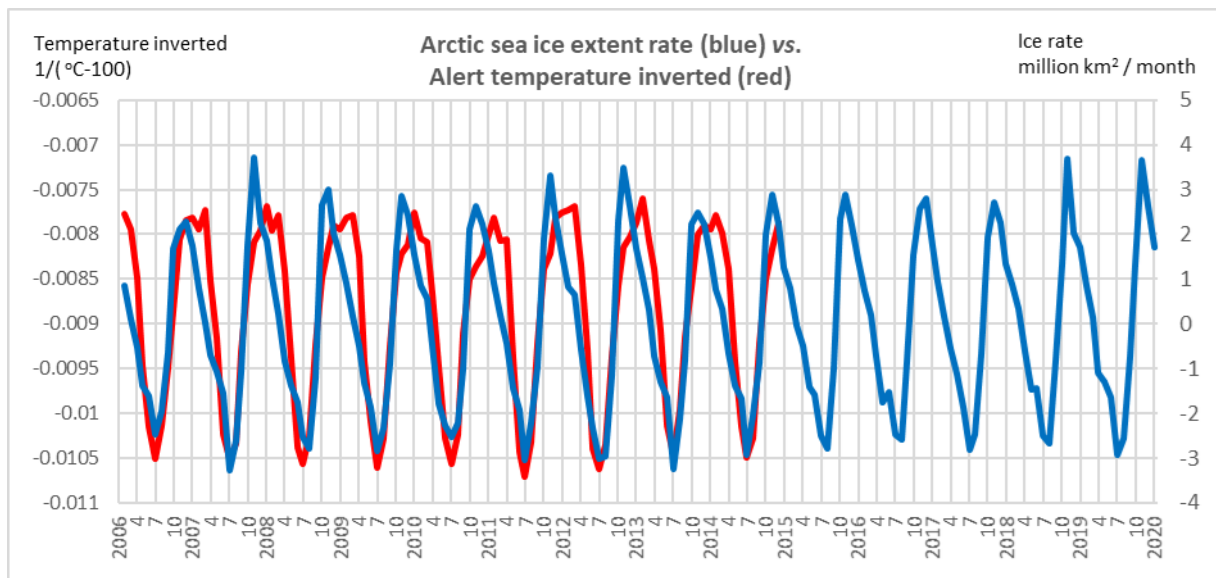


141  
142 **Fig. 9** Monthly methane rate Alert vs. Northern Hemisphere snow extent rate

143

144 Time series for Arctic sea ice extent rate and a local temperature (Alert) are given in Fig. 10

145

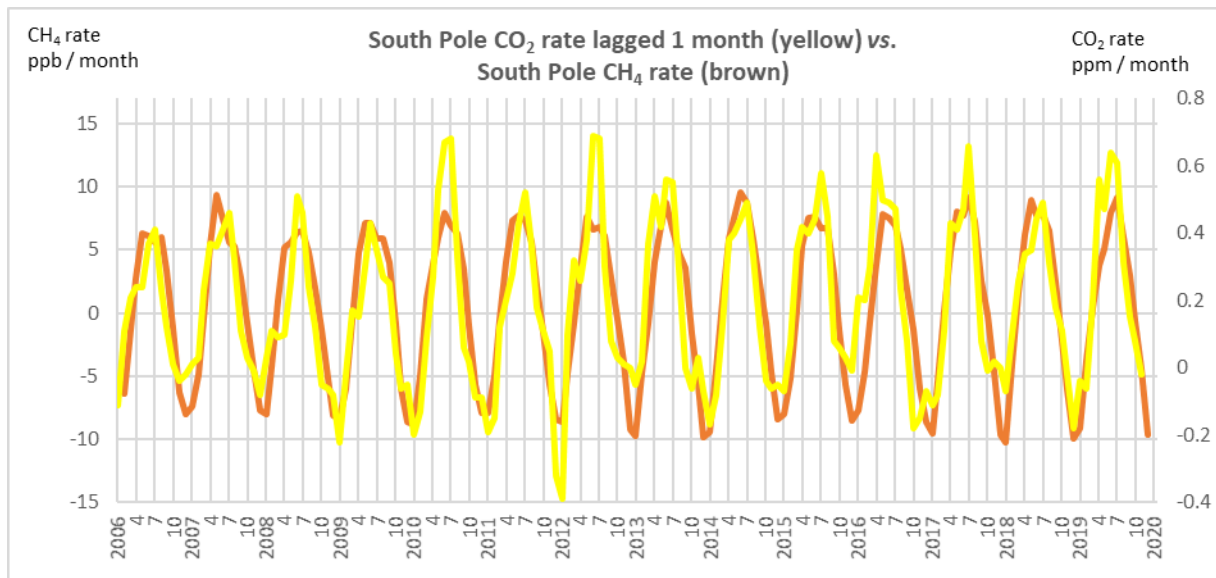


146  
147 **Fig. 10** Monthly Arctic sea ice extent rate vs. temperature at Alert (inverted)

148

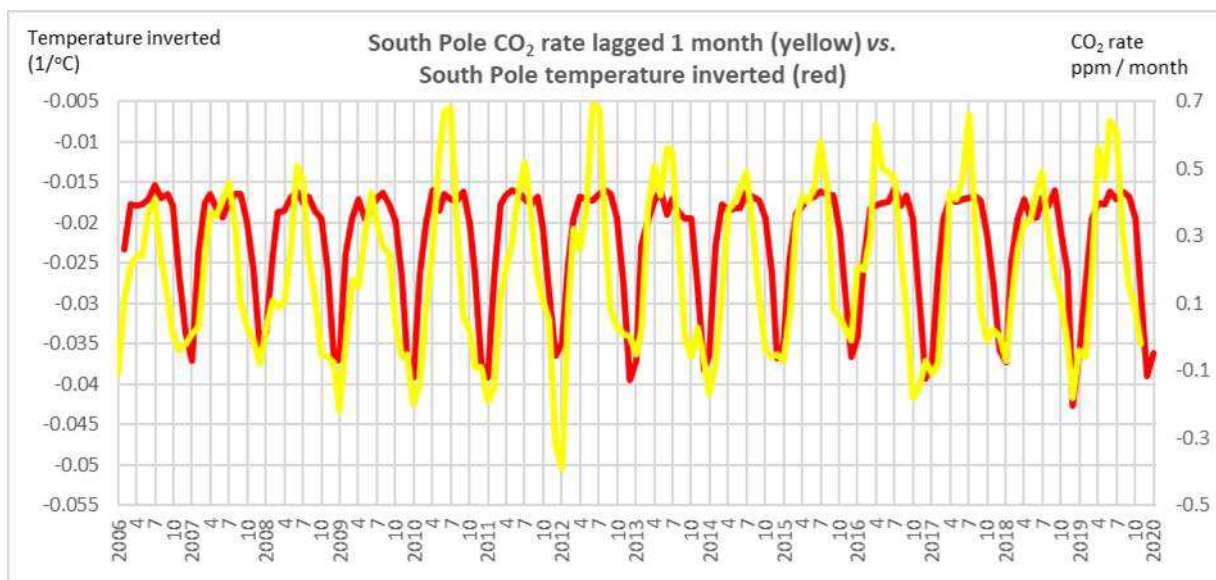
149 **c) Antarctic**

150 Monthly time series of carbon dioxide rate and methane rate at the South Pole, and temperature at the South Pole, are  
151 given in Figs. 11 - 13.



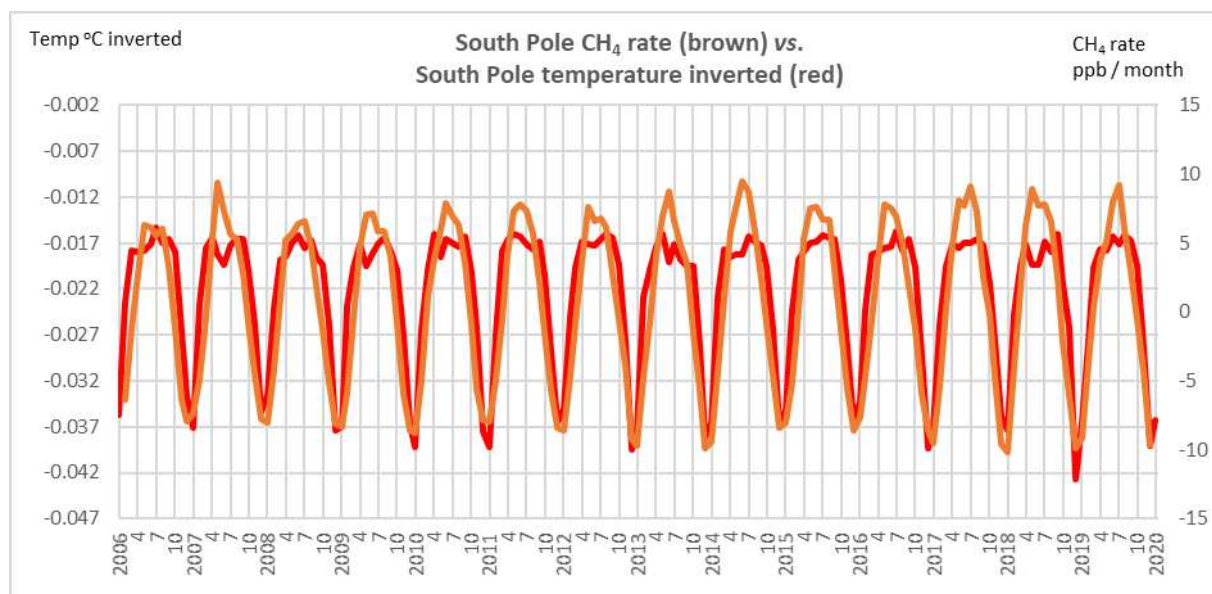
152  
153 **Fig. 11** Monthly carbon dioxide rate South Pole (lagged 1 month) vs. monthly methane rate South Pole

154



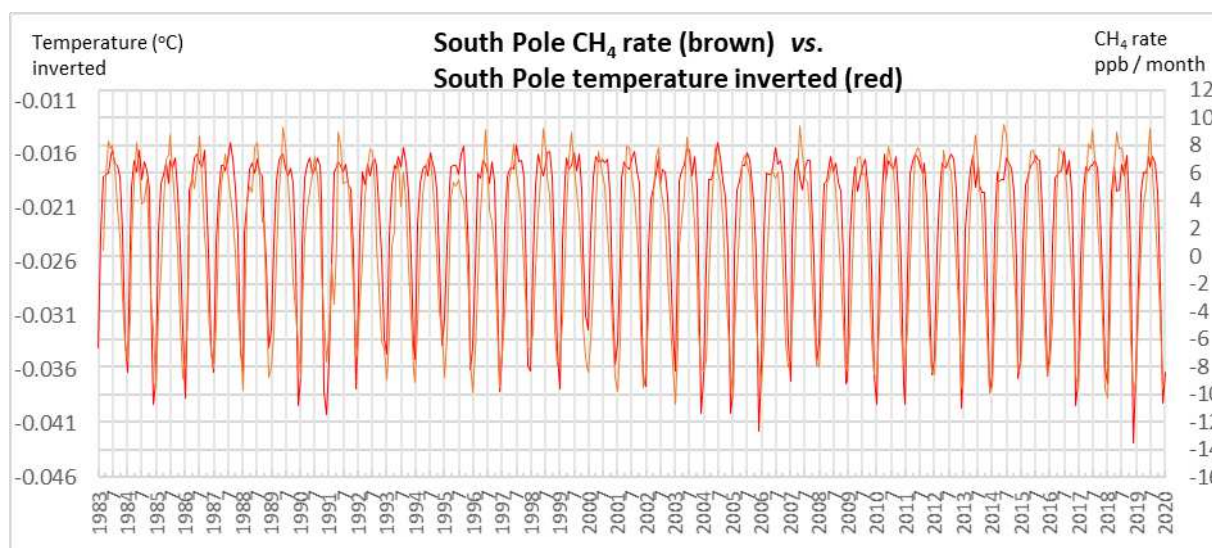
155  
156 **Fig. 12** Monthly carbon dioxide rate South Pole (lagged 1 month) vs. temperature at South Pole (inverted)

157



158  
159 **Fig. 13a** Monthly methane rate South Pole vs. temperature at South Pole (inverted).  $r = 0.88$  at zero lag;  $p < 0.001$

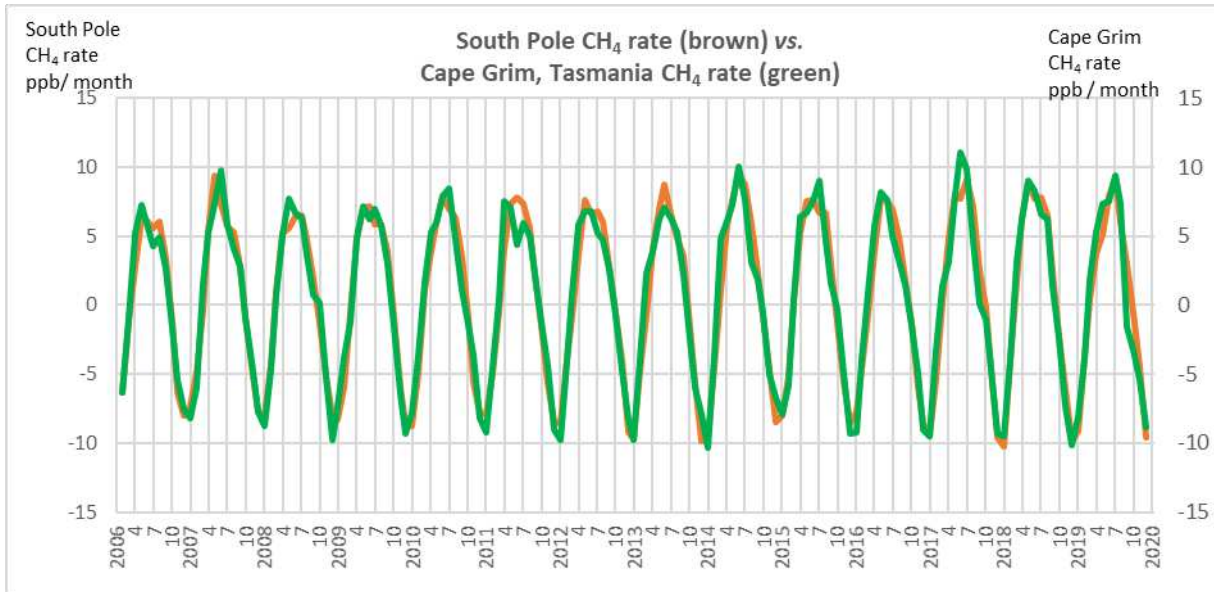
160



161  
162 **Fig. 13b** Monthly South Pole methane rate vs. temperature at South Pole (inverted), using full continuous monthly  
163 methane record from February 1983

164

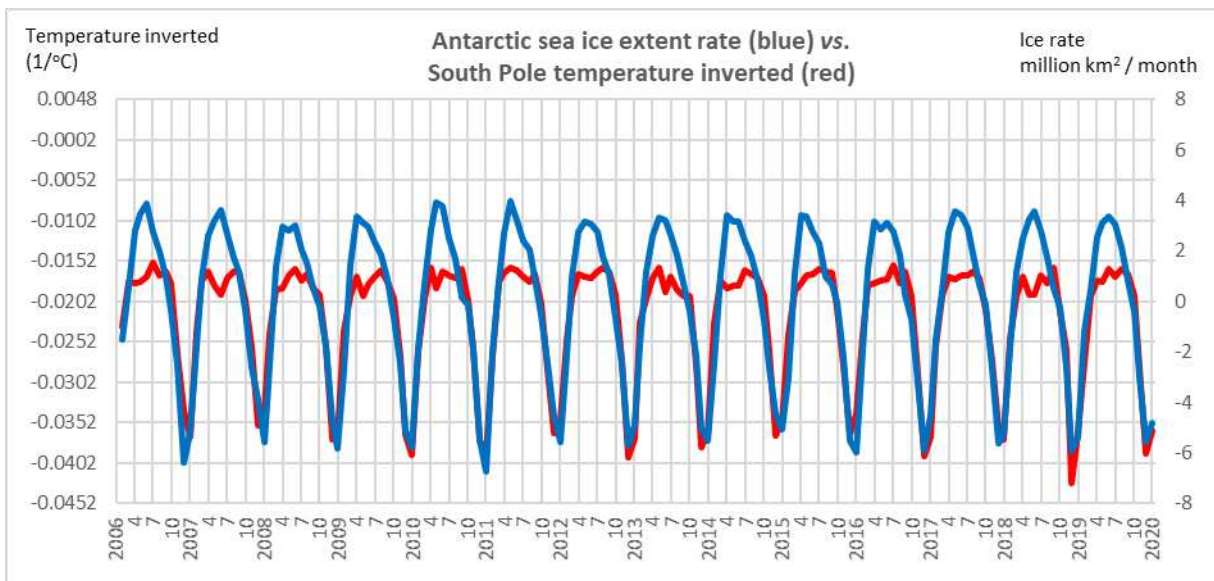
165 An example of the similarity of South Pole methane rate phenology to another Southern Hemisphere site, Cape  
166 Grim, is given in Fig. 14.



167  
168 **Fig. 14** Monthly methane rate South Pole vs. monthly methane rate Cape Grim (Tasmania)

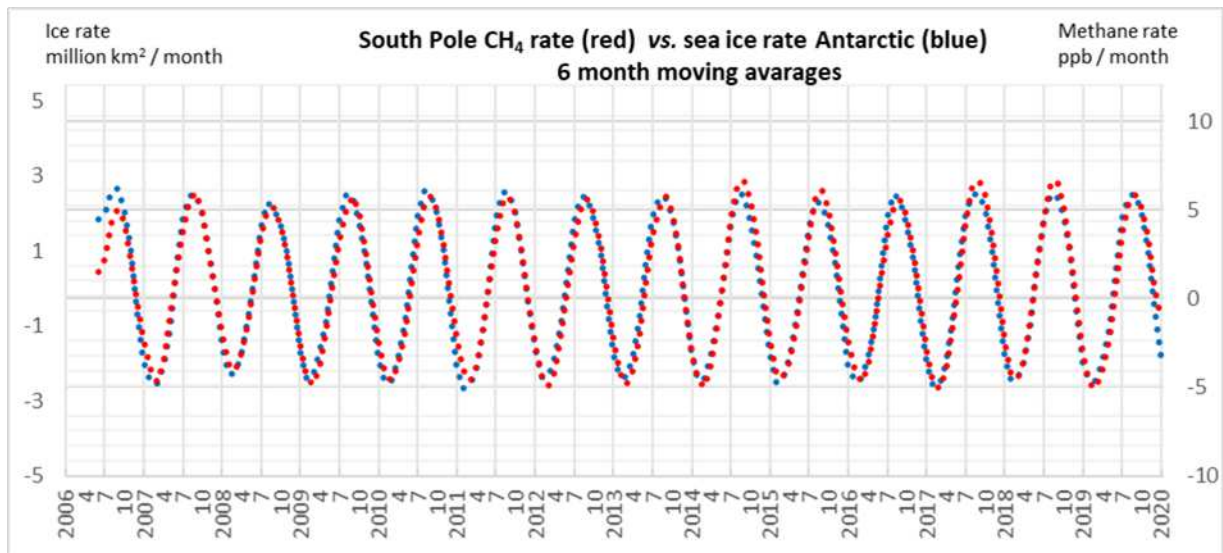
169

170 Time series for Antarctic sea ice rate, a local temperature and South Pole methane rate are given in Figs. 15 and 16.



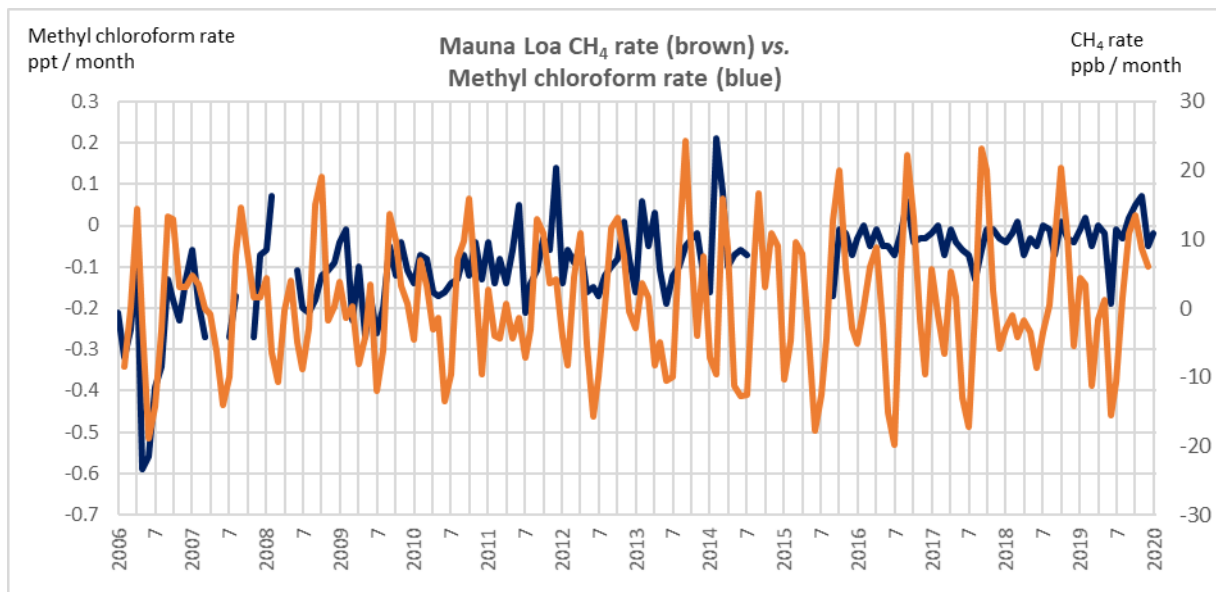
171  
172 **Fig. 15** Monthly Antarctic sea ice extent rate vs. temperature at South Pole (inverted)

173



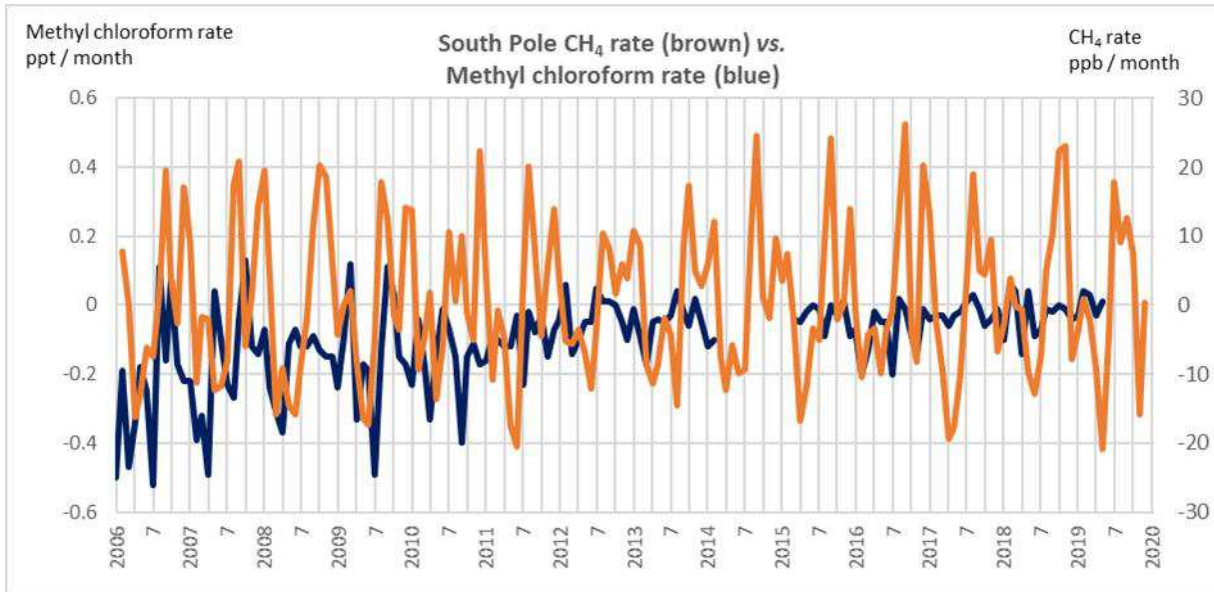
174  
175 **Fig. 16** Monthly Antarctic sea ice extent rate vs. monthly methane rate South Pole, 6 month moving average for both  
176 variables

177



178  
179 **Fig. 17a** Monthly methane rate Mauna Loa vs. monthly methyl chloroform rate Mauna Loa

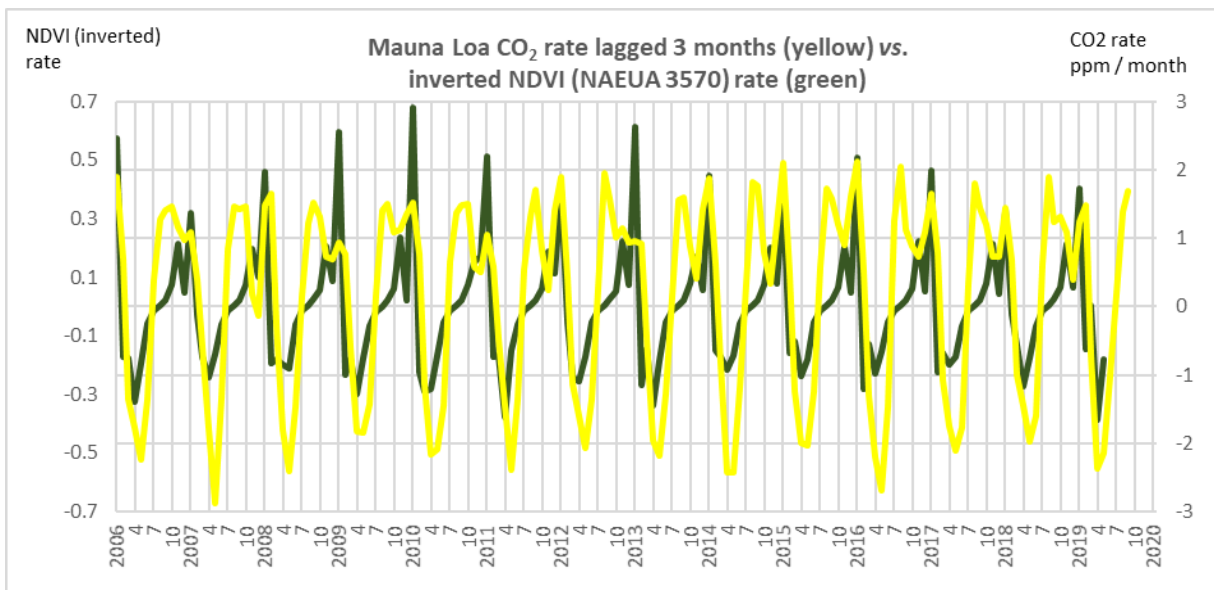
180



181  
182

**Fig. 17b** Monthly methane rate South Pole vs. monthly methyl chloroform rate South Pole

183

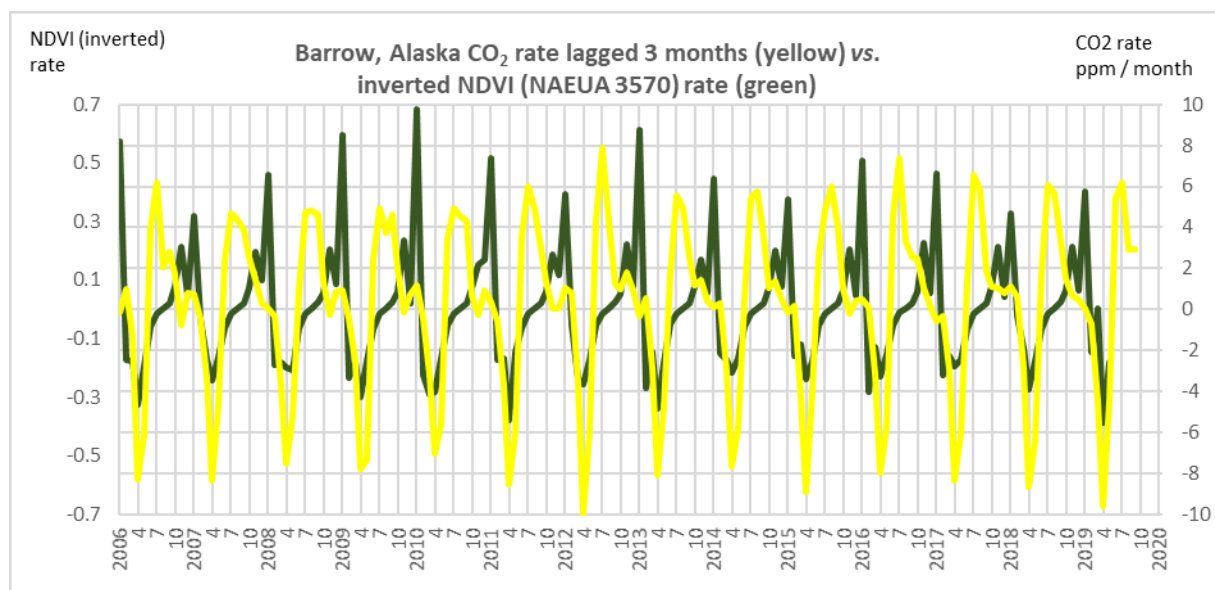


184  
185

**Fig. 18a** Monthly carbon dioxide rate Mauna Loa (20°N) lagged 3 months vs. monthly inverted NDVI rate North

186 America and Eurasia, 35°N to 70°N (NAEUA3570)

187



188 **Fig. 18b** Monthly carbon dioxide rate Barrow, Alaska (71°N) lagged 3 months vs. monthly inverted NDVI rate  
 189 North America and Eurasia, 35°N to 70°N (NAEUA3570)  
 190

191

192 **Discussion**

193 Air temperature at or near the Poles peaks in very close synchrony with regional peaks in sea ice melt (Figs. 10 and  
 194 15). It will also be correlated with a range of other abiotic and biotic variables with various lags, such as Northern  
 195 Hemisphere snow (Fig. 9) and Greenland terrestrial ice melt. Air temperature at high latitude sites leads the global  
 196 carbon dioxide rate with a greater lag of carbon dioxide behind the Antarctic than the Arctic temperature (Fig. 2 and  
 197 Fig. 3).

198

199 The rates of change of globally representative levels of carbon dioxide and methane are very strongly correlated with  
 200 the rate of change of global ('Arctic plus Antarctic') sea ice (Figs. 1 and 4). The rate of change of methane at Mauna  
 201 Loa has similar phenology but greater amplitude (Fig. 5). At the South Pole, methane rates are very highly  
 202 synchronous with Antarctic sea ice extent rates (Fig. 16), as are other regional methane rates (Hambler & Henderson  
 203 2020b). The lag of 5 - 7 months between the peak Antarctic temperature (and sea ice melt) and the fastest decline of  
 204 global methane and global carbon dioxide suggest a strong Antarctic influence on these gases (Fig. 1 and Fig. 4). It  
 205 may take months for the effects of temperature on gas flux in the Antarctic to reach the Northern Hemisphere.

206

207 The extremely strong predictive power of global total sea ice for carbon dioxide and methane is notable - revealing  
208 possible causality or high predictive power for the actual cause. The two peaks in global sea ice rate result from the  
209 peak temperatures in the two Hemispheres. Global carbon dioxide and methane rates also have twin peaks which are  
210 similarly separated (Fig. 6). We propose that whatever dominates the fluxes of these gases makes strong  
211 contributions at high latitudes in both Hemispheres. For carbon dioxide we propose (on the basis of seasonal  
212 amplitudes and lags) that there is a particularly strong contribution from sea ice melt and calcium carbonate  
213 dissolution in the Greenland area (Hambler & Henderson 2020a).

214

215 Temperature in at least one Arctic recording site has a close synchrony with carbon dioxide (Fig. 7) and methane  
216 (Fig. 8) flux rates at the site (Alert, Canada). Other high-latitude Northern Hemisphere recording sites in the NOAA  
217 network have similar carbon dioxide and methane phenology to Alert (Hambler & Henderson, 2020a, b). Peak  
218 negative carbon dioxide flux (indicating drawdown or destruction of the gas) usually occurs synchronously with peak  
219 atmospheric temperature in the Arctic summer (July, Fig. 7). This is also synchronous with peak decline in Arctic  
220 ice extent (Fig. 10). However, peak negative methane flux at Alert (Fig. 8) occurs about one month earlier than peak  
221 temperature and peak sea ice melt in the whole Arctic, which we suggest results from an influence of the biota or  
222 other abiotic factors on methane dynamics in the Arctic. Arctic sea ice as a whole can not be the dominant causal  
223 variable in this region at least, but there are regional differences in sea ice phenology, and Alert methane peak  
224 decline is more closely synchronous with the Barents Sea ice rate (Hambler & Henderson, unpublished). Peak rate  
225 of decline of Arctic methane is also closely synchronous with peak snow extent decline in the Northern Hemisphere,  
226 with Alert lagging snow melt rate by about a month (Fig. 9), consistent with putative terrestrial influences such as  
227 increased methanogenic microbial activity. Peak methane emission from Arctic mires can occur near peak summer  
228 air temperature (Jackowicz-Korczyński et al 2010).

229

230 Peak negative methane flux at the South Pole is synchronous with peak temperature at the South Pole (Fig. 13) but  
231 carbon dioxide rate at the South Pole lags one month behind the peak temperature which occurs December / January  
232 (Fig. 12). Similarly, methane rates slightly lead carbon dioxide rates globally and at Mauna Loa (Figs. 4 - 6).  
233 Intriguingly, South Pole temperature peaks simultaneously with peak rates of decline in both methane and carbon  
234 dioxide at the coastal and marine Antarctic sites in the NOAA network (Palmer, Syowa, Halley, Drake Passage) and  
235 is also simultaneous with peak Antarctic sea ice melt (Hambler & Henderson, 2020a, b). There may be differential

236 transport, production or removal processes for methane and carbon dioxide after a synchronous monthly pattern is  
237 imprinted in the two gases at the edge of the Antarctic continent. High latitude sites in the Southern Hemisphere  
238 have very similar methane phenology (*e.g.* Fig. 14 and Hamblen & Henderson 2020b) suggesting a very well-mixed  
239 southern air mass (as per Dlugokencky et al 1994) and / or a large-scale causal process.

240

241 The synchronous decline and rise in carbon dioxide and methane at many sites would most parsimoniously be  
242 explained by a single mechanism. These results are broadly consistent with our proposals that sea ice is either  
243 involved in the decline of atmospheric carbon dioxide and methane or is extremely strongly correlated with an  
244 unknown variable causing fluxes of the gases (Hamblen & Henderson 2020a, b). We argue the extremely high  
245 correlations between sea ice and fluxes of both gases are more plausibly due to simple physical or chemical  
246 processes than to ecological ones (Hamblen & Henderson 2020a, b). In particular, we suggest the peak negative gas  
247 rates may relate to ice melt and absorption by cold water undersaturated in these gases (Wiesenburg & Guinasso Jr  
248 1979). Similarly, ocean temperature was suggested to drive lagged carbon dioxide changes through solubility  
249 changes (Park 2009). The peak positive rates may relate to expulsion of gas during sea ice formation (degassing),  
250 marine emissions, and other physical and biological processes (Hamblen & Henderson 2020a, b). Mechanisms  
251 coupling sea ice and the atmosphere (such as brine drainage, modulation of upwelling, and ikaite dissolution cycles)  
252 are not yet well represented qualitatively or quantitatively in biogeochemical models (Kort et al 2012; Damm et al  
253 2015; Vancoppenolle & Tedesco 2017) and their magnitudes may have been underestimated.

254

255 The conventional explanation of the terrestrial biota of the Northern Hemisphere driving the carbon dioxide seasonal  
256 cycle (Keeling et al 1989; Keeling et al 2001, 2005; Buermann et al 2007; Keeling 2008; IPCC 2013; He et al  
257 2017; Jiang & Yung 2019) does not explain the similar patterns of global carbon dioxide and methane which have  
258 many different biological and abiotic sources and sinks (IPCC 2013). The similar patterns of seasonal variation of  
259 CO<sub>2</sub> concentration and <sup>13</sup>C isotopic fraction at several locations is puzzling if the fractionation mechanism is biotic  
260 and predominantly northern (Keeling et al 2005) but not if it is physical and the same in both Hemispheres. Isotopes  
261 are in any case of limited use in identifying carbon fluxes because different sources can have the same fractions  
262 (Salby 2012).

263

264 Measured by NDVI, terrestrial productivity has relatively weak synchrony and curve shape similarity with carbon  
265 dioxide rates, in any large region, even with lags (Fig.18; Hambler & Henderson 2020a), making this a less likely  
266 driver than sea ice rates despite common belief. For the period 2003-2018 inclusive, the cross correlation between  
267 sea ice volume and carbon dioxide rates ( $r = 0.90$ ) is stronger than between NDVI (35°N -70 °N) and carbon dioxide  
268 rates ( $r = 0.62$ ), Hambler & Henderson (2020a). Alternatively, NDVI may be of limited value in detecting carbon  
269 fixation rates despite its conventional use for this purpose - and dependence of flux on precipitation or other factors  
270 affecting productivity might be expected to introduce noise and weaken the relationship further. Terrestrial fluxes of  
271 carbon dioxide are not as well known as many imagine, and much recent data has been surprising - as with periods of  
272 emission from tropical forests or large fluxes over deserts (*e.g.* Mearns 2015; Qin et al 2021). Those supporting the  
273 conventional 'consensus' view have yet to locate areas of the planet with such strong correlations as we find with  
274 global carbon dioxide rates - yet probably have an intuitive feeling such areas exist since this is easier to accept than  
275 to reject the current paradigm.

276

277 A major factor implicated in removing atmospheric methane, the hydroxyl radical (OH) (Dlugokencky et al 1994;  
278 Mastepanov et al 2008; Salby 2012; Ciais et al 2013) is created by photodissociation and thus would be expected to  
279 be temperature-dependent with latitudinal variation in amplitude. Indeed, OH concentration is highest in the tropics  
280 (Hein et al 1997; Reidel & Lassey 2008). If as is widely assumed OH is dominant in global methane dynamics it  
281 would be expected to cause lagged fluxes of methane at the polar sites. The seasonal low of methane *level* near the  
282 South Pole occurs when OH is assumed high in the austral summer (Dlugokencky et al 1994). However, methane  
283 rate lags further behind peak temperature nearer the equator (Hambler & Henderson 2020b) suggesting net methane  
284 loss is not fastest where there is most sunlight. The relationship between methane rates and methyl chloroform rates  
285 is relatively weak (*e.g.* Fig. 17 and Hambler & Henderson, unpublished). Moreover, to our knowledge there is no  
286 reported directly causal reason for OH to vary synchronously with carbon dioxide rate (as it often does regionally).  
287 Indeed, the positive modelled correlation between marine methane emission and photosynthetic productivity (Weber  
288 et al 2019) would argue against synchrony with carbon dioxide release.

289

290 A lag of 7 months between temperature and carbon dioxide rate is consistent with the observed lag of about 9 - 10  
291 months between temperature and carbon dioxide level (Humlum et al 2013; Salby 2013), suggesting South Pole air  
292 temperature is a very good proxy for a variable driving the annual carbon cycle. South Pole air temperature and

293 Antarctic sea ice extent rate should both have predictive power for the 'global' carbon dioxide level 10 months in  
294 advance. Our results are consistent with a proposed sequence of events driving carbon dioxide changes starting in  
295 the Southern Hemisphere (Humlum et al 2013). Tropical ocean temperature anomaly is also significantly coherent  
296 with lagged carbon dioxide level (Park 2009); temperature fluctuations at gridpoints in North East America and the  
297 North Atlantic but not polar regions were also significantly coherent with Mauna Loa carbon dioxide fluctuations; it  
298 is possible the difference from our result reflects Park's use of the Hadley Centre's HadCrut3 temperature anomaly,  
299 rather than temperature, and carbon dioxide levels, rather than rates.

300

301 Critiques of our methods and conclusions might suggest that there are stronger terrestrial flux correlations with the  
302 gas rates that have yet to be identified, and that the recorded quantities (moles) of carbon dioxide or methane in sea  
303 ice are insufficient to cause the global flux changes. Our results are indeed inconsistent with current estimates of gas  
304 budgets (*e.g.* Dlugokencky et al 1994; Ciais et al 2013; Saunois et al 2020). Our response is that it is circular  
305 reasoning to use existing sampling of quantities and flux measurements to argue our predictions on under-sampled  
306 quantities must be wrong. Falsification of our hypotheses would require much more comprehensive spatial and  
307 temporal coverage of gas levels (such as satellites might provide). Whilst some carbon stores (such as in sea ice  
308 itself) might be lower than we predict, a combination of several temperature-dependent fluxes and stores in the  
309 carbon cycle might combine to reach the magnitudes required. Although sparse, many measurements of carbon  
310 dioxide phenology in polar regions show similar timings of positive and negative fluxes that are in general agreement  
311 with an involvement of sea ice and calcium carbonate (ikaite) dissolution (Hambler & Henderson 2020a). However,  
312 high temporal and spatial variability suggests determination of net annual flux from all regions will require hourly or  
313 daily, consistent sampling at large scales and more systematic analysis. Analyses and animations of the globe  
314 showing rates of change of gases, rather than levels, may be particularly informative and convincing.

315

316 Inter-annual variation in monthly rates leads to net accumulation or loss of methane and carbon dioxide from the  
317 atmosphere. Both the amplitude and phase of methane rates in many sites in the Southern Hemisphere south of about  
318 25°S are very similar (Hambler & Henderson 2020b, and *e.g.* Fig. 14) suggesting large-scale common forcing. A  
319 variable such as temperature which correlates strongly with the amplitude of the annual cycle (*e.g.* Fig. 13) could  
320 help explain net global trends: for example, warm years generally have higher sea ice melt rates and more negative  
321 gas rates which might be partially caused by dissolution in melt water and changes in upwelling of gas-laden water.

322 The monthly timeseries of sea ice extent we use (Table 1) are presumably created with relatively consistent methods  
323 between years but are only provided since 2006. There may be too little statistical power to examine in detail  
324 relationships between sea ice and annual rate - but Hambler & Henderson (2020a) demonstrate annual carbon  
325 dioxide rates correlate strongly with global and oceanic lower tropospheric temperature and thus mechanisms  
326 involving ice could be hypothesized. The selected longer timeseries we have examined do not suggest recent years  
327 are anomalous (Fig. 2c; Fig. 2d; Fig. 3c; and Fig.13b) and these warrant further analysis.

328

### 329 **Conclusions**

330 We suggest other variables be examined that might be influenced by temperature or insolation which might drive  
331 fluxes of carbon dioxide and methane. These include, for example, marine and terrestrial productivity, upwelling  
332 rates, sea temperature depth profiles, glacial and ice shelf melt and calving, winds, and the hydroxyl radical (for  
333 methane). Isolating the relative contributions of such factors would require far more data, although the sharp decline  
334 of atmospheric carbon dioxide and methane precisely at the time of peak ice melt suggests dissolution in temporarily  
335 cold water is a major component. However, our correlations between sea ice rates, carbon dioxide rates and methane  
336 rates are the strongest with a putative driver of global greenhouse gas dynamics that we are aware of - and we  
337 suggest they are a priority for further investigation and empirical tests of causality and mechanism. The global and  
338 Antarctic cycle of both gases have similarities suggesting the same processes or regions are involved in the dominant  
339 fluxes for both, despite their very different biological properties.

340

341 If temperature drives the annual cycle of carbon dioxide and methane it should be no surprise if variation in  
342 temperature between years causes changes in the annual rate of accumulation or decline of these gases (Hambler &  
343 Henderson 2020a, b). Variation in the shape of the monthly temperature curve (*e.g.* Fig. 3c) can be used to predict  
344 variation in the monthly change of the gases - and hence monthly levels. A common mechanism could cause the  
345 observed similarity of long term changes in these gases (Salby 2012, 2013). The phase relationship between  
346 temperature and carbon dioxide has been examined to help elucidate the possible direction of causality (Stips et al  
347 2016; Faes et al 2017) and the lags we find between time series are consistent with carbon dioxide being the  
348 response variable.

349

350 The current paradigm for the carbon cycle is supported by weaker correlations than the paradigm we propose.  
 351 Whilst paradigm shifts require strong evidence, a failure to thoroughly explore stronger correlations would be  
 352 scientifically negligent. If potential processes with appropriately large magnitudes are discovered though  
 353 correlations, large scale experiments will be needed to test causation. Given the high economic, social and  
 354 environmental costs (Hambler & Canney 2013) of attempting to manipulate the flux of greenhouse gases it is  
 355 paramount that natural fluxes be identified and partitioned to deduce the relative scale of human influence upon  
 356 them.

357

358 **Methods**

359 We use the datasets in Table 1.

Variable	Data source
Atmospheric CO <sub>2</sub>  Mauna Loa, Alert and South Pole  Monthly flask	NOAA GML Carbon Cycle Cooperative Global Air Sampling Network, 1983-2019, Version: 2020-07-24  <a href="https://www.esrl.noaa.gov/gmd/dv/data/">https://www.esrl.noaa.gov/gmd/dv/data/</a>  <a href="ftp://aftp.cmdl.noaa.gov/data/trace_gases/co2/flask">ftp://aftp.cmdl.noaa.gov/data/trace_gases/co2/flask</a>  Accessed 1 August 2020  Dlugokencky et al (2020a)
Atmospheric CH <sub>4</sub>  Atmospheric CH <sub>4</sub> (continued)  Mauna Loa, Alert, Cape Grim and South Pole  Monthly flask	NOAA GML Carbon Cycle Cooperative Global Air Sampling Network, 1983-2019, Version: 2020-07-24  <a href="https://www.esrl.noaa.gov/gmd/dv/data/">https://www.esrl.noaa.gov/gmd/dv/data/</a>  <a href="ftp://aftp.cmdl.noaa.gov/data/trace_gases/ch4/flask">ftp://aftp.cmdl.noaa.gov/data/trace_gases/ch4/flask</a>  Accessed 1 August 2020  Dlugokencky et al (2020b)
Atmospheric CH <sub>4</sub>  Globally-averaged monthly data	<a href="https://esrl.noaa.gov/gmd/ccgg/trends_ch4/">https://esrl.noaa.gov/gmd/ccgg/trends_ch4/</a>  Accessed 1 January 2021  Dlugokencky (2021)
Atmospheric methyl chloroform  Gas chromatograph hourly samples	Methyl chloroform data from the NOAA/ESRL halocarbons in situ program  <a href="https://www.esrl.noaa.gov/gmd/dv/data/">https://www.esrl.noaa.gov/gmd/dv/data/</a>  Accessed 29 March 2021
NDVI	MDOIS satellite imagery MOD13C2 product as 5 kilometre monthly mean global imagery  Accessed July 2019

<p><i>Table 1 continued.</i></p> <p>Sea ice extent</p> <p>Monthly mean</p>	<p><a href="https://nsidc.org/data/seaice_index/archives">https://nsidc.org/data/seaice_index/archives</a></p> <p>Sea Ice Index Version 3 <a href="ftp://sidads.colorado.edu/DATASETS/NOAA/G02135/">ftp://sidads.colorado.edu/DATASETS/NOAA/G02135/</a> (Fetterer et al 2017)</p> <p>'North' (= 'Arctic'): <a href="ftp://sidads.colorado.edu/DATASETS/NOAA/G02135/north/monthly/data/">ftp://sidads.colorado.edu/DATASETS/NOAA/G02135/north/monthly/data/</a> at <a href="http://sidads.colorado.edu">sidads.colorado.edu</a></p> <p>'South' (= 'Antarctic'): <a href="ftp://sidads.colorado.edu/DATASETS/NOAA/G02135/south/monthly/data/">ftp://sidads.colorado.edu/DATASETS/NOAA/G02135/south/monthly/data/</a></p> <p>Files in form: S_01_extent_v3.0.csv</p> <p>Accessed 26 February 2020</p>
<p>Snow extent</p> <p>Northern Hemisphere</p> <p>Snow extent (continued)</p> <p>Monthly mean</p>	<p><a href="https://climate.rutgers.edu/snowcover/docs.php?target=datareq">https://climate.rutgers.edu/snowcover/docs.php?target=datareq</a></p> <p>NH SCE CDR v01r01</p> <p><a href="https://climate.rutgers.edu/snowcover/files/moncov.namgnld.txt">https://climate.rutgers.edu/snowcover/files/moncov.namgnld.txt</a></p> <p><a href="https://climate.rutgers.edu/snowcover/files/moncov.nam.txt">https://climate.rutgers.edu/snowcover/files/moncov.nam.txt</a></p> <p>Accessed 27 March 2020</p>
<p>Alert air temperature</p> <p>Monthly mean</p>	<p>NCEP Reanalysis Dataset</p> <p>Produced at NOAA Physical Sciences laboratory</p> <p><a href="https://psl.noaa.gov/data/timeseries/arctic/">https://psl.noaa.gov/data/timeseries/arctic/</a></p> <p>Accessed 6 January 2021</p>
<p>South Pole air temperature</p> <p>(Amundsen-Scott South Pole Station)</p> <p>Monthly mean</p>	<p>Amundsen_Scott temperature</p> <p><a href="https://legacy.bas.ac.uk/met/READER/surface/Amundsen_Scott.All.temperature.txt">https://legacy.bas.ac.uk/met/READER/surface/Amundsen_Scott.All.temperature.txt</a></p> <p>British Antarctic Survey. UK Antarctic Surface Meteorology; 1947 - 2013</p> <p><a href="http://dx.doi.org/10.5285/569d53fb-9b90-47a6-b3ca-26306e696706">http://dx.doi.org/10.5285/569d53fb-9b90-47a6-b3ca-26306e696706</a></p> <p>Accessed 16 December 2020</p>

360 **Table 1** Data sources

361

362 We examine atmospheric gas levels for a site considered globally representative for carbon dioxide (Mauna Loa,  
 363 Hawaii, USA) (IPCC 2013), and a global average estimate of monthly methane (Dlugokencky 2021). We also  
 364 examine methane rates at Mauna Loa since these are measurements from what might also be a representative site for  
 365 methane.

366

367 Within the NOAA Global Monitoring Laboratory network of atmospheric gas recording sites we examine the most  
 368 northerly site (Alert, Canada) and the most southerly (South Pole) since these would be predicted to respond strongly

369 to any temperature-dependent forcing. Having examined all sites in this network with monthly flask data we selected  
370 Cape Grim (Tasmania, Australia, latitude 41°S) as an illustration of the high similarity of phenology of the South  
371 Pole to some sites at lower latitudes.

372

373 We do not use models of atmospheric transport of gas but instead make the minimalistic assumption that gas from a  
374 polar region will take longer to reach or cross the equator than to reach nearby sites. We assume the shape of the  
375 seasonal gas flux curve will be most similar to the curve of the causal variable near the site of the causal variable  
376 (due to mixing).

377

378 Temperature data (average monthly values in degrees Centigrade) were obtained for meteorological stations at the  
379 South Pole and Alert as examples of very high-latitude sites where local gas levels are also monitored. The Alert  
380 data were rescaled by subtracting 100, to make all values negative. Temperature values were inverted to visually  
381 compare synchrony of peak temperature with peak negative net fluxes of the gases, since we have previously  
382 established peak negative flux is tightly synchronous with sea ice melt at high latitudes (Hambler & Henderson  
383 2020a, b).

384

385 Recording of the OH radical in the atmosphere is very difficult, so is usually done indirectly using methyl  
386 chloroform ( $\text{CH}_3\text{CCl}_3$ ) which OH reacts with and hence lowers the atmospheric concentration (Ravishankara &  
387 Albritton 1995; Hein et al 1997; Reidel & Lassey 2008). In the annual cycle, low levels of methyl chloroform  
388 should correspond to high levels of OH.

389

390 We follow the classic use of NDVI to locate likely carbon dioxide fluxes due to terrestrial vegetation productivity  
391 (Keeling et al 1989; Buermann et al 2007; He et al 2017). There is high synchrony in monthly NDVI rates between  
392 the Northern Hemisphere latitudinal belts and continents (Hambler and Henderson 2020a) and thus for simplicity of  
393 presentation we selected data for North America and Eurasia, 35°N to 70°N, which has high amplitude (as does  
394 recorded carbon dioxide flux at northern high latitudes) and which captures a substantial area of these continents.  
395 Use of NDVI for the full Northern Hemisphere or a narrower high latitude belt would not affect our conclusions  
396 (Hambler & Henderson 2020a). We invert monthly data for NDVI to give an approximate measure of a lack of

397 productivity (indicating periods which have a net carbon dioxide sink). These are rescaled by a factor of 1000 for  
398 clarity.

399

400 Methodological consistency is essential in time series analysis (Henderson 2021) so we use datasets which are very  
401 likely to have been quality controlled for methodological drift. A monthly database of sea ice extent is easily  
402 available from NSIDC from January 2006, which we therefore use as the start date. Arctic and Antarctic extents  
403 were used to calculate the rate for the 'global' sea ice extent (which we term 'Arctic plus Antarctic' rate as in Hambler  
404 & Henderson 2020a, b). Longer timeseries are available and presented for selected variables, such as the full  
405 continuous carbon dioxide record at Mauna Loa from July 1976, to visually assess if more recent years have a very  
406 different pattern.

407

408 Rates of change for variables were derived as follows: rate in month 2 is the mean value in month 2 minus the mean  
409 value in month 1.

410

411 Statistical analysis was based on the R platform. Cross correlations and consideration of autocorrelation were  
412 performed as in Hambler & Henderson (2020b). For pairs of time series, cross correlations and 95% confidence  
413 bounds for lags of up to +/- 12 months were calculated using the ccf function in the tseries R package. These results  
414 were used to identify the lag producing the highest correlation and the rcorr function then used to calculate the  
415 Pearson correlation and associated probability that it could be generated by random chance. Because we find  
416 probabilities are near zero for numerous of our results, which would require many digits to present, significance  
417 values are all presented as  $p < 0.001$ .

418

419 Due to data availability and other constraints at the time of this work, some time series have different end dates or  
420 missing values so are not fully comparable and not all are analysed statistically. Statistical analyses are only  
421 performed here for the global levels of methane and carbon dioxide and for one other time series for illustrative  
422 purposes (showing a tight visual fit is also supported statistically). The results of any analysis are given in the Figure  
423 captions. Previous work (Hambler & Henderson 2020a, b and unpublished) has established that close visual fits

424 using the minima in such time series always have high statistical correlations and often identify the lag between  
425 them; this can be confirmed if the work is replicated.

426

#### 427 **Data availability Statement**

428 Data are available from the sources in Table 1.

429

#### 430 **References**

431 Buermann, W., Lintner, B.R., Koven, C.D. et al (2007) The changing carbon cycle at Mauna Loa Observatory.

432 *Proceedings of the National Academy of Sciences*, **104**, 4249-4254.

433 Bushinsky, S.M., Landschützer, P., Rödenbeck, C. et al (2019) Reassessing Southern Ocean air sea CO<sub>2</sub> flux

434 estimates with the addition of biogeochemical float observations. *Global Biogeochemical Cycles*, **33**, 1370-

435 1388.

436 Ciais, P., Sabine, C., Bala, G. et al (2013) Carbon and other biogeochemical cycles. In: *Climate change 2013: the*

437 *physical science basis. Contribution of Working Group I to the Fifth Assessment Report of the*

438 *Intergovernmental Panel on Climate Change* (ed. by T. Stocker, D. Qin, G.-K. Plattner et al), pp. 465-570.

439 Cambridge University Press, Cambridge, United Kingdom.

440 Damm, E., Rudels, B., Schauer, U. et al (2015) Methane excess in Arctic surface water - triggered by sea ice

441 formation and melting. *Scientific Reports*, **5**, 16179.

442 Dlugokencky, E. J., Steele, L., Lang, P. M. et al (1994) The growth-rate and distribution of atmospheric methane.

443 *Journal of Geophysical Research: Atmospheres*, **99**, 17021-17043.

444 Dlugokencky, E.J., Mund, J.W., Crotwell, A.M. et al (2020a) Atmospheric carbon dioxide dry air mole fractions

445 from the NOAA GML Carbon Cycle Cooperative Global Air Sampling Network, 1968-2019, Version:

446 2020-07. <https://doi.org/10.15138/wkgj-f215>. Accessed 1 August 2020.

447 Dlugokencky, E.J., Crotwell, A.M., Mund, J.W. et al (2020b) Atmospheric methane dry air mole fractions from the

448 NOAA GML Carbon Cycle Cooperative Global Air Sampling Network, 1983-2019, Version: 2020-07,

449 <https://doi.org/10.15138/VNCZ-M766>. Accessed 1 August 2020.

450 Dlugokencky, E. (2021) Ed Dlugokencky, NOAA/GML ([www.esrl.noaa.gov/gmd/ccgg/trends\\_ch4/](http://www.esrl.noaa.gov/gmd/ccgg/trends_ch4/)). Accessed 1

451 January 2021.

452 Faes, L., Nollo, G., Stramaglia, S. et al (2017) Multiscale granger causality. *Physical Review E*, **96**, 042150.

- 453 Fung, I., John, J., Lerner, J. et al (1991) Three-dimensional model synthesis of the global methane cycle. *Journal of*  
454 *Geophysical Research*, **96**, 13033-13065.
- 455 Geilfus, N.-X., Pind, M., Else, B. et al (2018) Spatial and temporal variability of seawater  $p\text{CO}_2$  within the Canadian  
456 Arctic Archipelago and Baffin Bay during the summer and autumn 2011. *Continental Shelf Research*, **156**,  
457 1-10.
- 458 Hamblen, C. & Canney, S.M. (2013) *Conservation*. Cambridge University Press, Cambridge, United Kingdom.
- 459 Hamblen, C. & Henderson, P.A. (2020a) Sea ice and carbon dioxide. Working Paper, version 2.  
460 <https://ora.ox.ac.uk/objects/uuid:640a0c7e-6b55-4aff-a9cc-f47f6b490254>
- 461 Hamblen, C. & Henderson, P.A. (2020b) Sea ice and methane. Working paper, version 2.  
462 <https://ora.ox.ac.uk/objects/uuid:52b0e80f-7358-4b88-8941-55068738638e>.
- 463 He, Z.H., Zeng, Z.C., Lei, L.P. et al (2017[https://ora.ox.ac.uk/objects/uuid:52b0e80f-7358-4b88-8941-](https://ora.ox.ac.uk/objects/uuid:52b0e80f-7358-4b88-8941-55068738638e)  
464 [55068738638e](https://ora.ox.ac.uk/objects/uuid:52b0e80f-7358-4b88-8941-55068738638e)) A data-driven assessment of biosphere-atmosphere interaction impact on seasonal cycle  
465 patterns of XCO<sub>2</sub> Using GOSAT and MODIS observations. *Remote Sensing*, **9**, 251.
- 466 Hein, R., Crutzen, P. J. & Heimann, M. (1997) An inverse modelling approach to investigate the global atmospheric  
467 methane cycle. *Global Biogeochemical Cycles*, **11**, 43-76.
- 468 Henderson, P.A. (2021). *Southwood's Ecological Methods*. 5th Edn. Oxford University Press, Oxford, United  
469 Kingdom.
- 470 Humlum, O., Stordahl, K. & Solheim, J.-E. (2013) The phase relation between atmospheric carbon dioxide and  
471 global temperature. *Global and Planetary Change*, **100**, 51-69.
- 472 IPCC (2013) *Climate Change 2013: The physical science basis. Contribution of Working Group I to the Fifth*  
473 *Assessment Report of the Intergovernmental Panel on Climate Change* (ed. by T. Stocker, D. Qin, G.-K.  
474 Plattner et al), Cambridge University Press, Cambridge, United Kingdom.
- 475 Jackowicz-Korczyński, M., Christensen, T.R., Bäckstrand, K. et al (2010) Annual cycle of methane emission from a  
476 subarctic peatland. *Journal of Geophysical Research*, **115**, G02009.
- 477 Jiang, X. & Yung, Y.L. (2019) Global patterns of carbon dioxide variability from satellite observations. *Annual*  
478 *Review of Earth and Planetary Sciences*, **47**, 225-245.
- 479 Keeling, C.D., Bacastow, R.B., Carter, A. et al (1989) A three-dimensional model of atmospheric CO<sub>2</sub> transport  
480 based on observed winds: 4. Mean annual gradients and interannual variations. *Aspects of climate*  
481 *variability in the Pacific and the Western Americas*, **55**, 305-363.
- 482 Keeling, C.D., Piper, S.C., Bacastow, R.B. et al (2005). Atmospheric CO<sub>2</sub> and <sup>13</sup>CO<sub>2</sub> exchange with the terrestrial  
483 biosphere and oceans from 1978 to 2000: observations and carbon cycle implications. In EPRINTS-BOOK-

- 484 TITLE University of Groningen, Centre for Isotope Research.
- 485 Keeling, C.D., Piper, S.C., Bacastow, R.B. et al (2001) Exchanges of atmospheric CO<sub>2</sub> and <sup>13</sup>CO<sub>2</sub> with the terrestrial  
486 biosphere and oceans from 1978 to 2000. In: *Exchanges of atmospheric CO<sub>2</sub> and <sup>13</sup>CO<sub>2</sub> with the terrestrial*  
487 *biosphere and oceans from 1978 to 2000. I. Global aspects, SIO Reference Series, No. 01-06*, pp. 1-88.  
488 Scripps Institution of Oceanography, San Diego.
- 489 Keeling, R.F. (2008) Recording Earth's vital signs. *Science*, **319**, 1771-1772.
- 490 Kort, E. A., Wofsy, S. C., Daube, B. C. et al (2012) Atmospheric observations of Arctic Ocean methane emissions up  
491 to 82 degrees north. *Nature Geoscience*, **5**, 318-321.
- 492 Mastepanov, M., Sigsgaard, C., Dlugokencky, E.J. et al (2008) Large tundra methane burst during onset of freezing.  
493 *Nature*, **456**, 628–630.
- 494 Mearns, E. (2015). CO<sub>2</sub> - The view from space - update. <http://euanmearns.com/co2-the-view-from-space-update/>  
495 Accessed 24 April 2021.
- 496 MOSAiC (2019) The key to the Arctic puzzle. From <https://www.mosaic-expedition.org/science/arctic-climate/>.  
497 Accessed 29 October 2019.
- 498 Park, J. (2009) A re-evaluation of the coherence between global-average atmospheric CO<sub>2</sub> and temperatures at  
499 interannual time scales. *Geophysical Research Letters*, **36**, L22704.
- 500 Qin, Y, Xiao, X., Wigneron, J.-P. et al (2021) Carbon loss from forest degradation exceeds that from deforestation in  
501 the Brazilian Amazon. *Nature Climate Change* (2021), <https://doi.org/10.1038/s41558-021-01026-5>.
- 502 Ravishankara, A.R. & Albritton, D.L. (1995) Methyl chloroform and the atmosphere. *Science*, **269**, 183-184.
- 503 Reidel, K. & Lassey, K. (2008) "Detergent of the atmosphere". *Water & Atmosphere*, **16**, 22-23.
- 504 Resplandy, L., Keeling, R., Rödenbeck, C. et al (2018) Revision of global carbon fluxes based on a reassessment of  
505 oceanic and riverine carbon transport. *Nature Geoscience*, **11**, 504-509.
- 506 Salby, M. (2012) *Physics of the atmosphere and climate*, 2nd edn. Cambridge University Press, Cambridge, United  
507 Kingdom.
- 508 Salby, M. (2013) Presentation Prof. Murry Salby in Hamburg on 18 April 2013.  
509 [https://www.youtube.com/watch?v=2ROw\\_cDKwc0&feature=youtu.be](https://www.youtube.com/watch?v=2ROw_cDKwc0&feature=youtu.be). Accessed 9 February 2021.
- 510 Saunio, M., Stavert, A. R., Poulter, B. et al (2020) The Global Methane Budget 2000-2017. *Earth System Science*  
511 *Data*, **12**, 1561-1623.
- 512 Sitch, S., Friedlingstein, P., Gruber, N. et al (2015) Recent trends and drivers of regional sources and sinks of carbon  
513 dioxide. *Biogeosciences*, **12**, 653-679.
- 514 Stips, A., Macias, D., Coughlan, C. et al (2016) On the causal structure between CO<sub>2</sub> and global temperature.

515 *Scientific Reports*, **6**, 1-9.

516 Vancoppenolle, M. & Tedesco, L. (2017) Numerical models of sea ice biogeochemistry. In: *Sea ice*, 3rd edn. (ed. by  
517 D.N. Thomas), pp. 492-515. Wiley, New Jersey.

518 Weber, T., Wiseman, N. A. & Kock, A. (2019) Global ocean methane emissions dominated by shallow coastal  
519 waters. *Nature Communications*, **10**, 4584.

520 Wiesenburg, D.A. & Guinasso Jr, N.L. (1979) Equilibrium solubilities of methane, carbon monoxide, and hydrogen  
521 in water and sea water. *Journal of Chemical and Engineering Data*, **24**, 356-360.

522 Winkler, A.J., Myneni, R.B., Alexandrov, G.A. et al (2019) Earth system models underestimate carbon fixation by  
523 plants in the high latitudes. *Nature Communications*, **10**, 1-8.

524 Zhao, F., Zeng, N., Asrar, G. et al (2016) Role of CO<sub>2</sub>, climate and land use in regulating the seasonal amplitude  
525 increase of carbon fluxes in terrestrial ecosystems: a multimodel analysis. *Biogeosciences*, **13**, 5121–5137.

526

527

## 528 **Acknowledgements**

529 Download and processing of MODIS satellite imagery was implemented by Environmental Research Group Oxford,  
530 Ltd. and we thank William Wint for this and for critical comment. Several colleagues and particularly Marian  
531 Dawkins provided valuable critiques. We thank all sources listed in Table 1 or indicated in the metadata on the  
532 hosting websites.

533

## 534 **Author Contributions**

535 CH and PAH contributed equally.

536

## 537 **Declarations**

538 **Funding** None.

539 **Conflict of interest / Competing Interest Statement** The authors have no conflict of interest / competing interests.

540 **Data Availability Statement** Data are available from the online providers indicated in Table 1. R code can be  
541 provided upon reasonable request.

542 **Figure Legends**

543 **Fig. 1** Global monthly carbon dioxide rate (measured at Mauna Loa, lagged 7 months) vs. global sea ice extent rate.

544  $r = 0.79$  at lag = 7 months;  $p < 0.001$

545 **Fig. 2a** Monthly carbon dioxide rate Mauna Loa (lagged 1 month) vs. temperature at Alert (inverted)

546 **Fig. 2b** Monthly carbon dioxide rate Mauna Loa (lagged 1 months) vs. temperature at Alert, Canada (inverted), 6

547 month moving average for both variables

548 **Fig. 2c** Monthly carbon dioxide rate Mauna Loa (lagged 1 month) vs. temperature at Alert, Canada (inverted), using

549 full continuous monthly Mauna Loa CO<sub>2</sub> record from July 1976

550 **Fig. 2d** Monthly carbon dioxide rate Mauna Loa (lagged 1 month) vs. temperature at Alert, Canada (inverted), 6

551 month moving average for both variables, using full continuous monthly Mauna Loa CO<sub>2</sub> record from July 1976

552 **Fig. 3a** Monthly carbon dioxide rate Mauna Loa (lagged 7 months) vs. temperature at South Pole (inverted)

553 **Fig. 3b** Monthly carbon dioxide rate Mauna Loa (lagged 7 months) vs. temperature at South Pole (inverted), 6

554 month moving average for both variables

555 **Fig. 3c** Monthly carbon dioxide rate Mauna Loa (lagged 7 months) vs. temperature at South Pole (inverted), using

556 full continuous monthly Mauna Loa CO<sub>2</sub> record from July 1976

557 **Fig. 4** Monthly global average methane rate (lagged 5 months) vs. global sea ice extent rate.  $r = 0.78$  at lag = 5

558 months;  $p < 0.001$

559 **Fig. 5** Monthly methane rate Mauna Loa (lagged 5 months) vs. global sea ice extent rate

560 **Fig. 6** Global carbon dioxide rate (Mauna Loa, lagged 2 months) vs. global methane rate

561 **Fig. 7** Monthly carbon dioxide rate Alert vs. temperature at Alert (inverted)

562 **Fig. 8** Monthly methane rate Alert vs. temperature at Alert (inverted)

563 **Fig. 9** Monthly methane rate Alert vs. Northern Hemisphere snow extent rate

564 **Fig. 10** Monthly Arctic sea ice extent rate vs. temperature at Alert (inverted)

565 **Fig. 11** Monthly carbon dioxide rate South Pole (lagged 1 month) vs. monthly methane rate South Pole

- 566 **Fig. 12** Monthly carbon dioxide rate South Pole (lagged 1 month) vs. temperature at South Pole (inverted)
- 567 **Fig. 13a** Monthly methane rate South Pole vs. temperature at South Pole (inverted).  $r = 0.88$  at zero lag;  $p < 0.001$
- 568 **Fig. 13b** Monthly South Pole methane rate vs. temperature at South Pole (inverted), using full continuous monthly
- 569 methane record from February 1983
- 570 **Fig. 14** Monthly methane rate South Pole vs. monthly methane rate Cape Grim (Tasmania)
- 571 **Fig. 15** Monthly Antarctic sea ice extent rate vs. temperature at South Pole (inverted)
- 572 **Fig. 16** Monthly Antarctic sea ice extent rate vs. monthly methane rate South Pole, 6 month moving average for both
- 573 variables
- 574 **Fig. 17a** Monthly methane rate Mauna Loa vs. monthly methyl chloroform rate Mauna Loa
- 575 **Fig. 17b** Monthly methane rate South Pole vs. monthly methyl chloroform rate South Pole
- 576 **Fig. 18a** Monthly carbon dioxide rate Mauna Loa (20°N) lagged 3 months vs. monthly inverted NDVI rate North
- 577 America and Eurasia, 35°N to 70°N (NAEUA3570)
- 578 **Fig. 18b** Monthly carbon dioxide rate Barrow, Alaska (71°N) lagged 3 months vs. monthly inverted NDVI rate
- 579 North America and Eurasia, 35°N to 70°N (NAEUA3570)
- 580 **Table 1** Data sources
- 581
- 582